Title: Particle Acceleration by Magnetic Reconnection in Striped Pulsar Winds and Relativistic Jets

Date: Mar 21, 2013 01:00 PM

URL: http://www.pirsa.org/13030078

Abstract: <span>The relativistic wind of pulsars consists of toroidal stripes of opposite magnetic field polarity, separated by current sheets of hot plasma. By means of 2D and 3D particle-in-cell simulations, we investigate particle acceleration and magnetic field dissipation at the termination shock of a striped pulsar wind. At the shock, the flow compresses and the alternating fields annihilate by driven magnetic reconnection. Irrespective of the stripe wavelength "lambda" or the wind magnetization "sigma" (in the regime sigma>>1 of magnetically-dominated flows), shock-driven reconnection transfers all the magnetic energy of the alternating fields to the particles. As the value of lambda/(r_L*sigma) increases (here, r_L is the relativistic Larmor radius in the wind), the post-shock spectrum passes from a thermal Maxwellian to a flat power-law tail with slope around -1.5, populated by particles accelerated by the reconnection electric field.

The limit lambda/(r_L*sigma)>>1 is realized in relativistic jets, where kink instabilities may seed the conditions for magnetic reconnection. Here, we find that the particle spectrum in the current sheet approaches a flat power-law tail with slope between -1.5 and -2, regardless of the conditions in the jet. The spectrum extends to higher energies for larger magnetizations or colder plasma temperatures, everything else being fixed. Our results place important constraints on the emission models of Pulsar Wind Nebulae and magnetically-dominated astrophysical jets.</span>

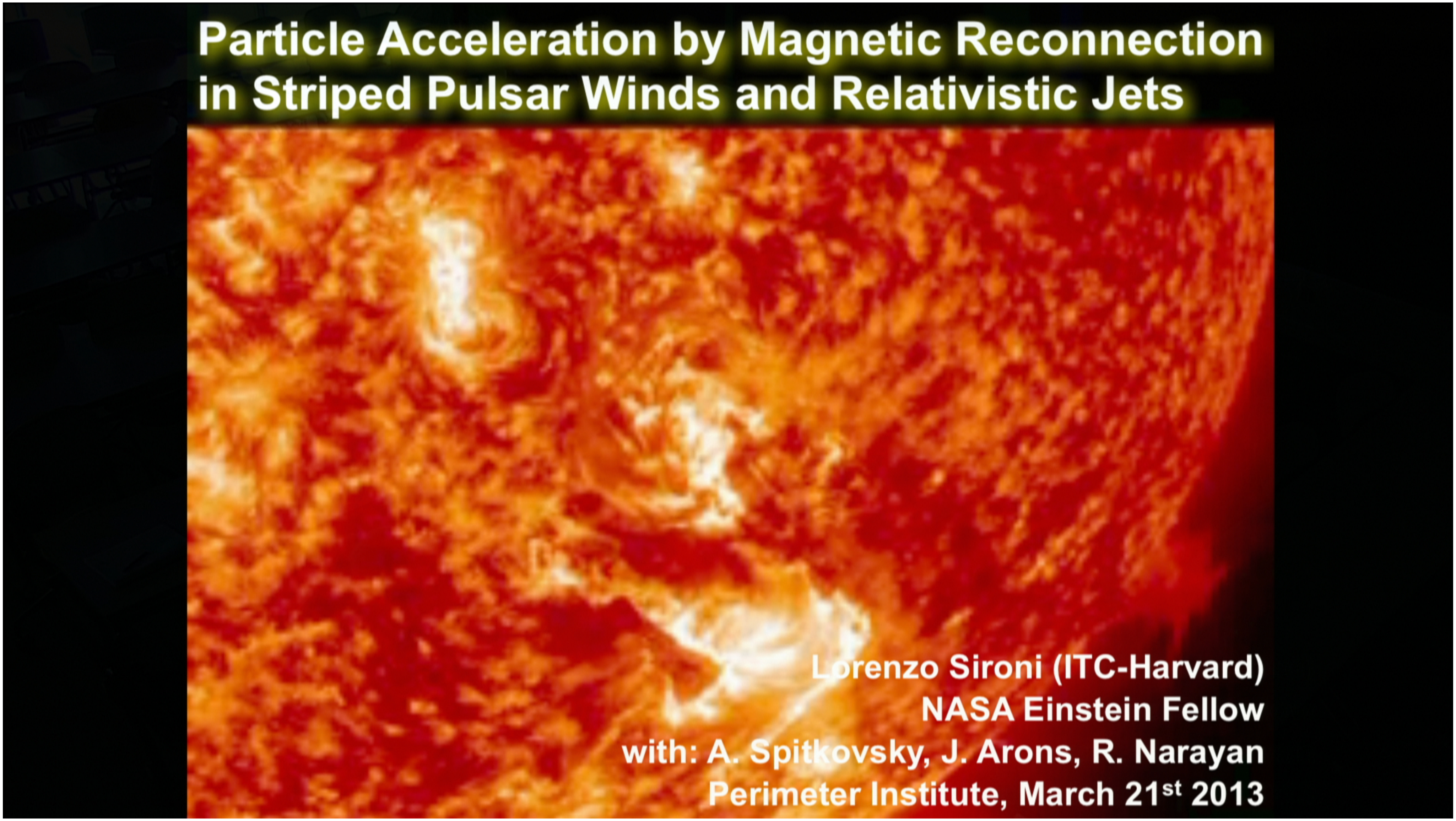
Particle Acceleration by Magnetic Reconnection in Striped Pulsar Winds and Relativistic Jets
Lorenzo Sironi (ITC-Harvard)
NASA Einstein Fellow
with: A. Spitkovsky, J. Arons, R. Narayan
Perimeter Institute, March 21st 2013

# Outline

- Non-thermal emission in Pulsar Wind Nebulae and relativistic jets.
- The physics of relativistic magnetic reconnection.
- Magnetic reconnection in striped pulsar winds and relativistic jets.
- The mechanism of particle acceleration in magnetic reconnection.
- Dependence on the flow properties.
- Astrophysical implications.

# Pulsars

Rotating magnetized neutron stars emitting pulsed radiation

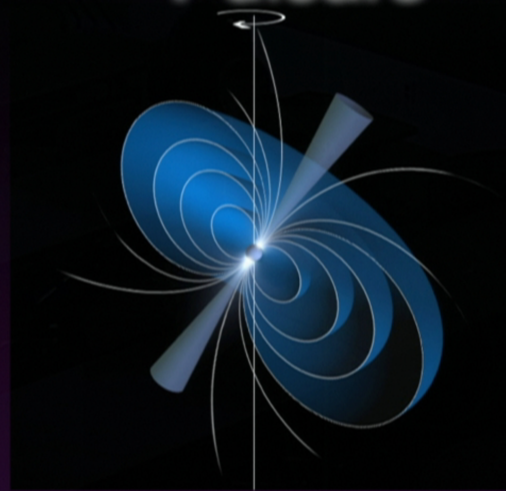

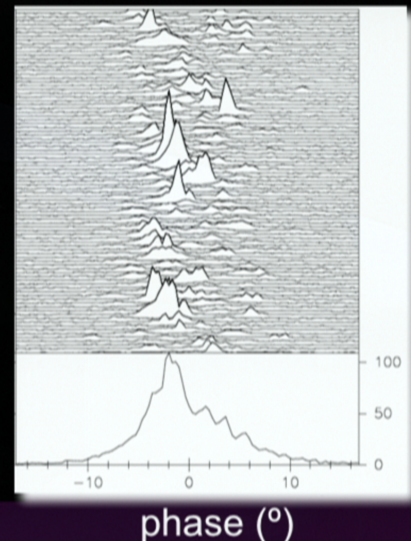

# Pulsars

Rotating magnetized neutron stars emitting pulsed radiation

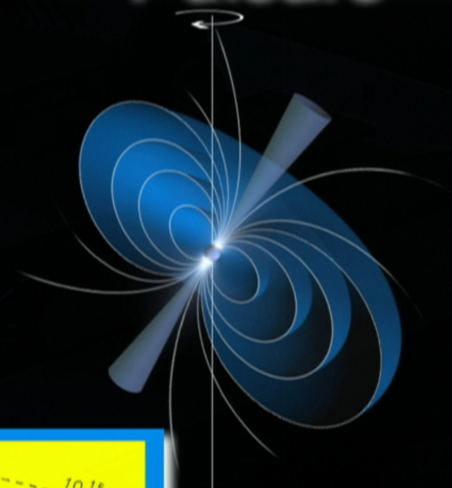

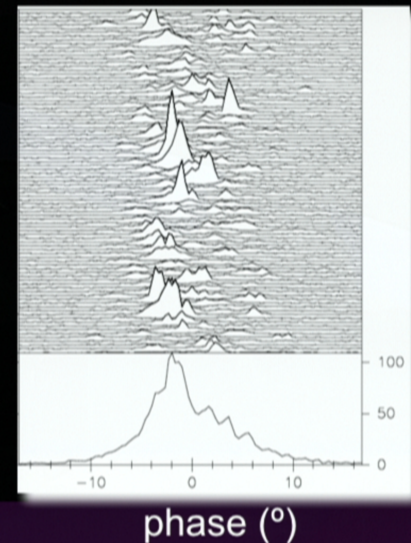


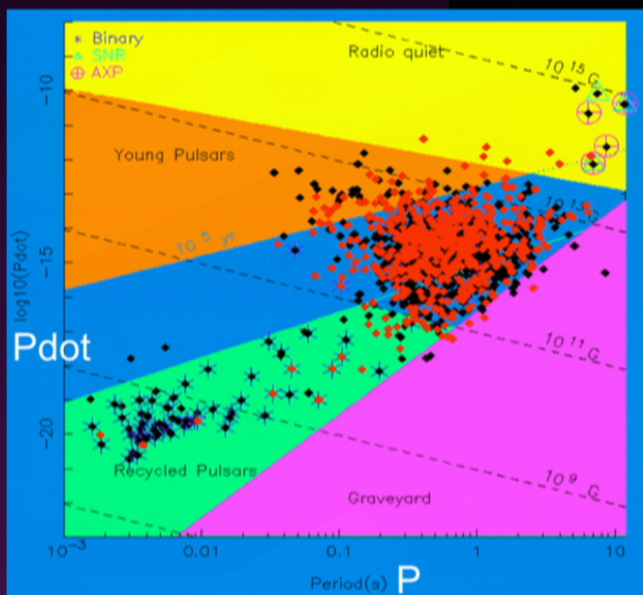


(Kramer et al 2003)

Main energy loss is invisible, but detectable: pulsars lose rotational kinetic energy!

Energy loss in radiation is a tiny fraction (0.01%-10%) of spin-down power

Energy loss leaves as a magnetized relativistic wind: Pulsar Wind

Where does the spin-down energy go?

# Non-thermal emission from PWNe

Crab Nebula

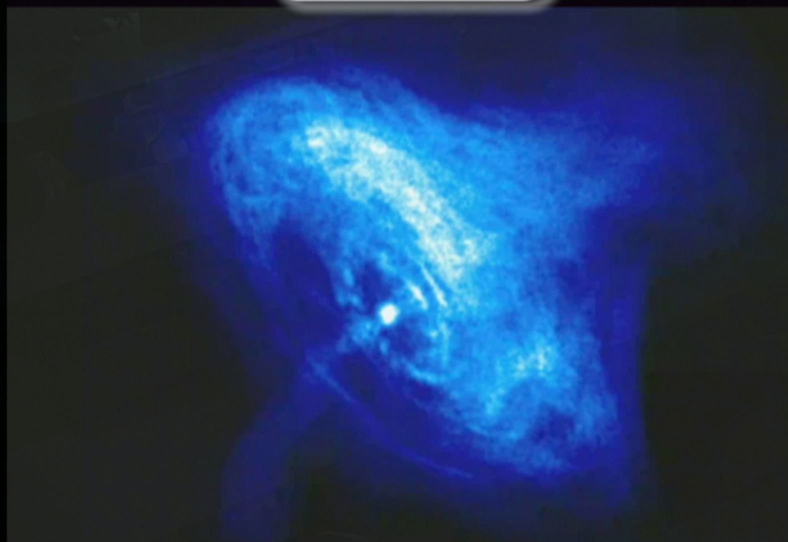

(Weisskopf et al 00)

Crab Nebula

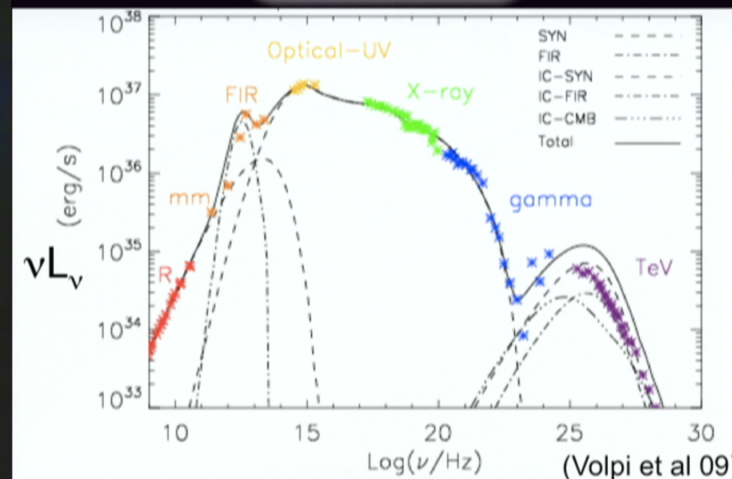


(Volpi et al 09)

- broadband spectrum, with two components (synchrotron + inverse Compton)
- flat radio slope ($L_\nu \propto \nu^{-0.3}$ for Crab), steep X-ray slope ($L_\nu \propto \nu^{-1.1}$ for Crab)
- high degree of linear radio and optical polarization → magnetic fields

# Magnetic reconnection 101

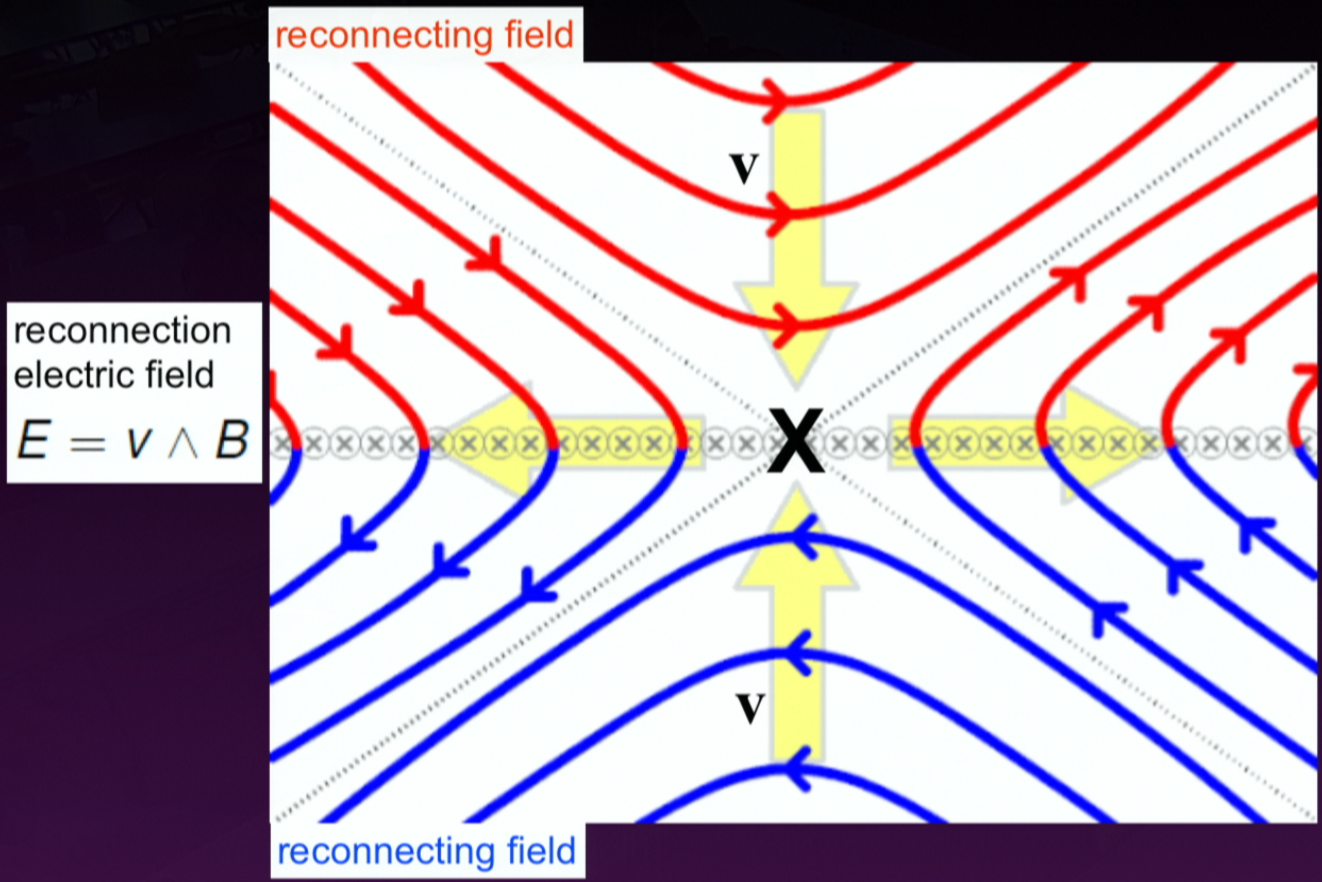


Reconnection happens because the plasma's electric resistivity near the boundary layer opposes the currents necessary to sustain the change in the magnetic field.

# Magnetic reconnection 101

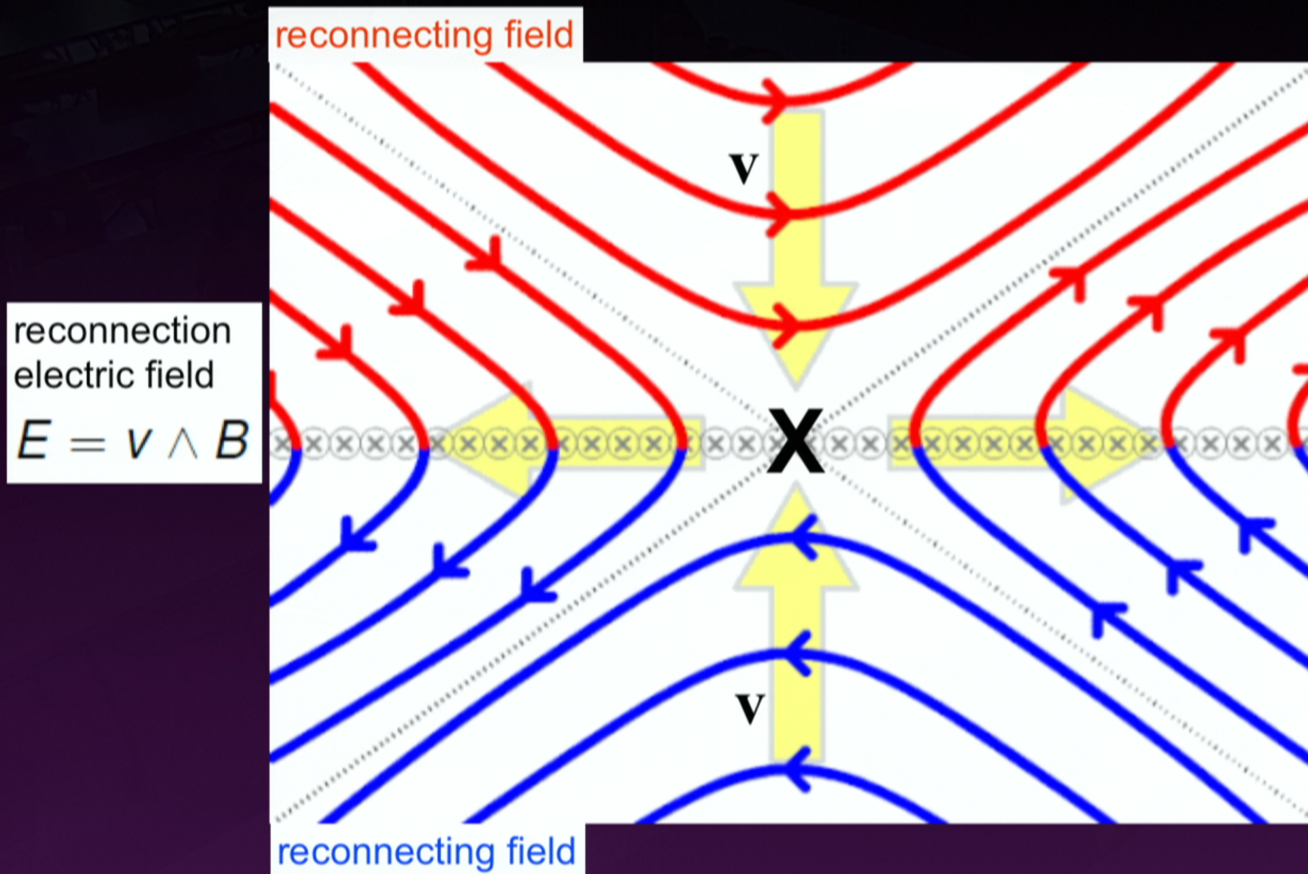


Reconnection happens because the plasma's electric resistivity near the boundary layer opposes the currents necessary to sustain the change in the magnetic field.

# Magnetic reconnection 101

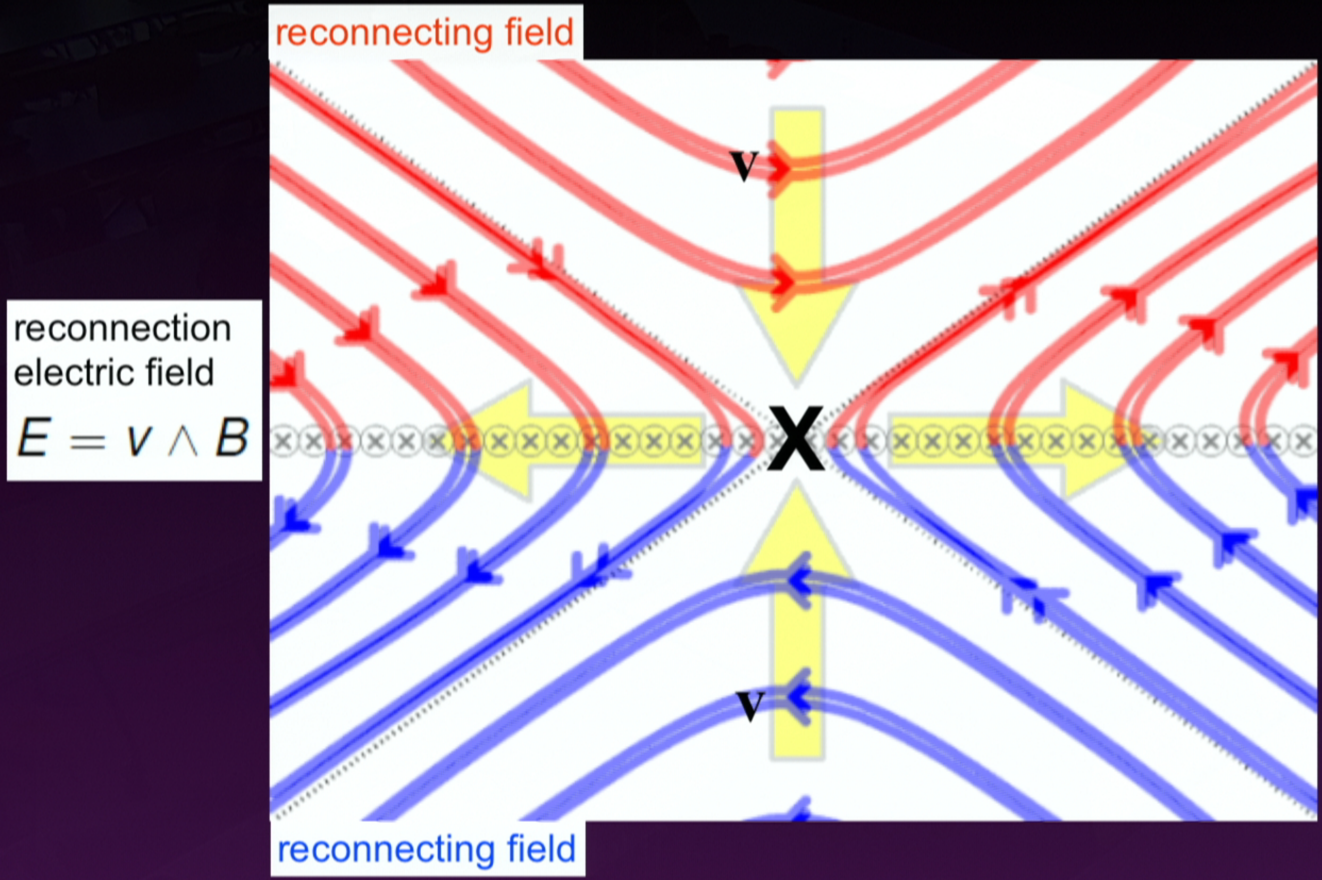


Reconnection happens because the plasma's electric resistivity near the boundary layer opposes the currents necessary to sustain the change in the magnetic field.

# Magnetic reconnection 501

- Can relativistic magnetic reconnection produce non-thermal power-law particle spectra?
- What is the slope $p$ of the non-thermal tail, such that

$$\frac{dn}{d\gamma} \propto \gamma^{-p}$$

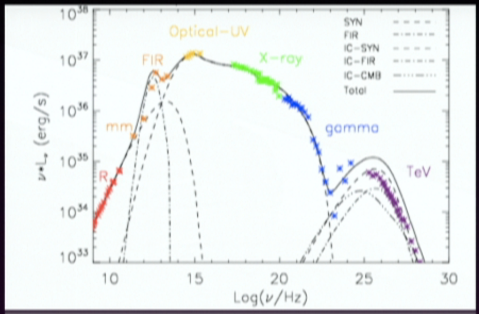

# Magnetic reconnection 501

- Can relativistic magnetic reconnection produce non-thermal power-law particle spectra?
- What is the slope $p$ of the non-thermal tail, such that

$$\frac{dn}{d\gamma} \propto \gamma^{-p}$$

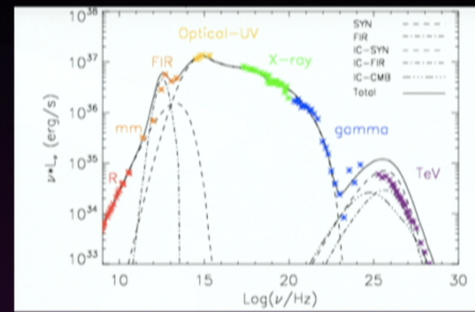


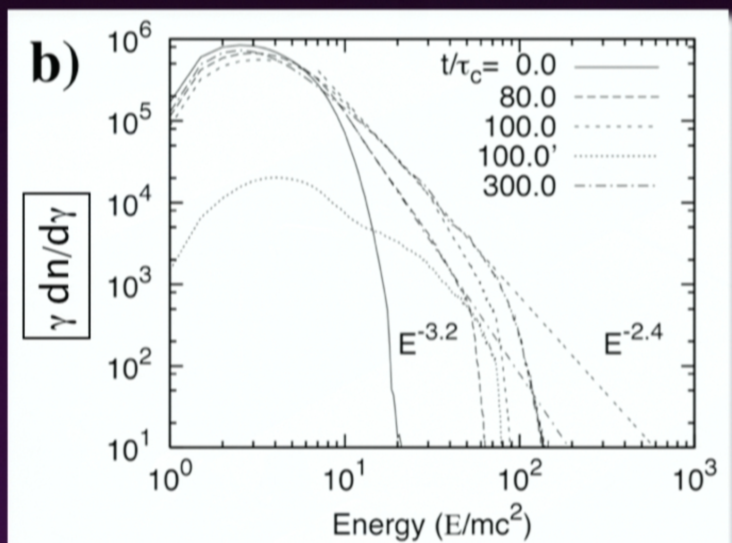


(Zenitani & Hoshino 07)

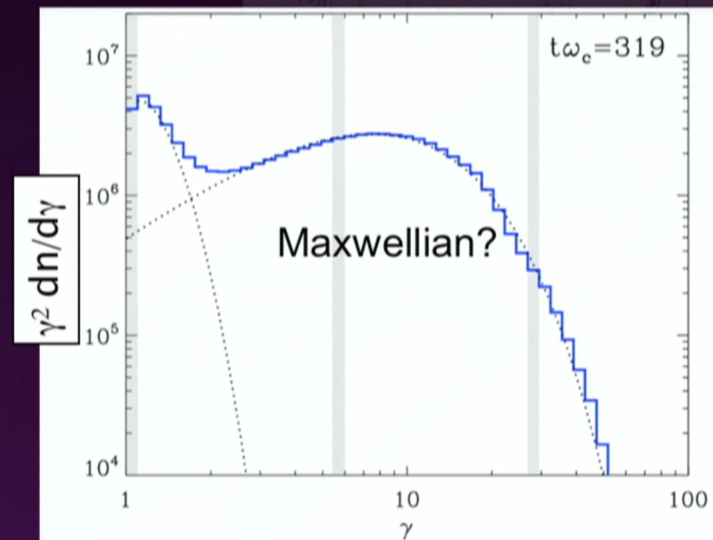


(Cerutti et al. 12)

# The PIC method

Particle-in-Cell (PIC) method:

1. Particle currents deposited on a grid

2. Electromagnetic fields solved on the grid via Maxwell's equations

3. Lorentz force interpolated to particle locations

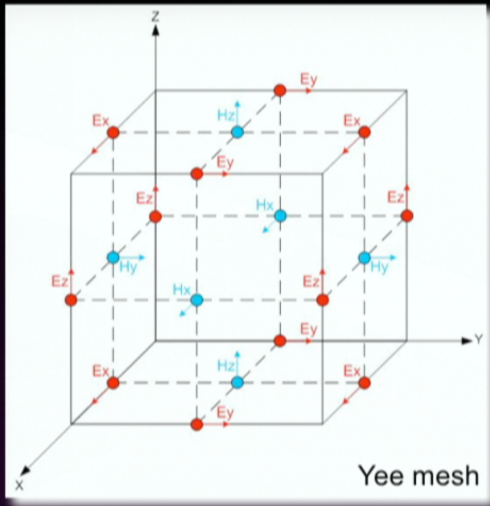

# The PIC method

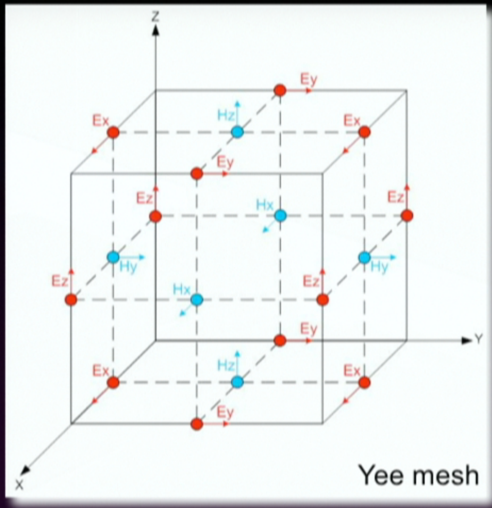


Particle-in-Cell (PIC) method:

1. Particle currents deposited on a grid

2. Electromagnetic fields solved on the grid via Maxwell's equations

3. Lorentz force interpolated to particle locations


No approximations, plasma physics at a fundamental level


Tiny length and time scales need to be resolved ➔ huge simulations, limited time coverage

- Relativistic 3D e.m. PIC code TRISTAN-MP (Buneman '93, Spitkovsky '05)

# Reconnection in pulsar winds & jets

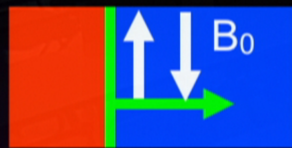


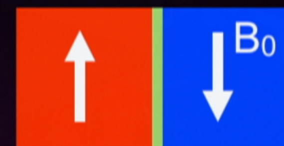


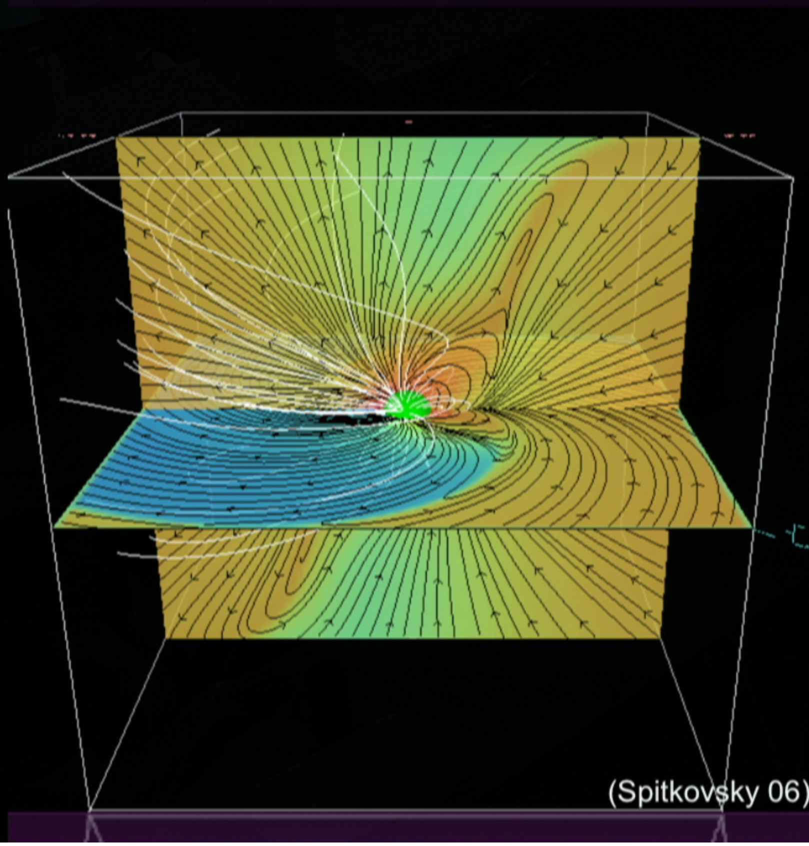

(Spitkovsky 06)

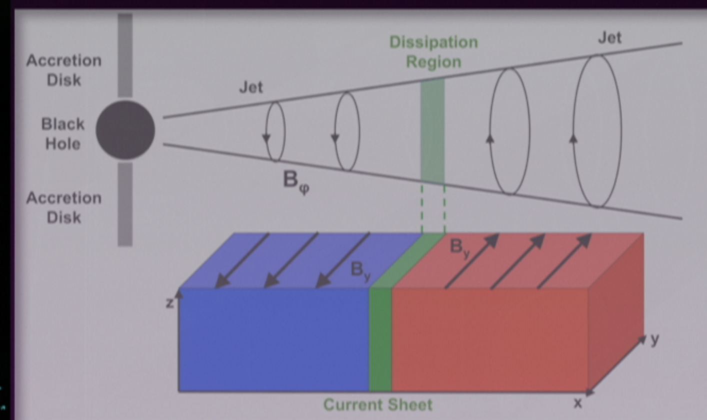

# Shock structure

$\sigma=10 \quad \lambda=320\ c/\omega_p \quad \alpha=0.1$

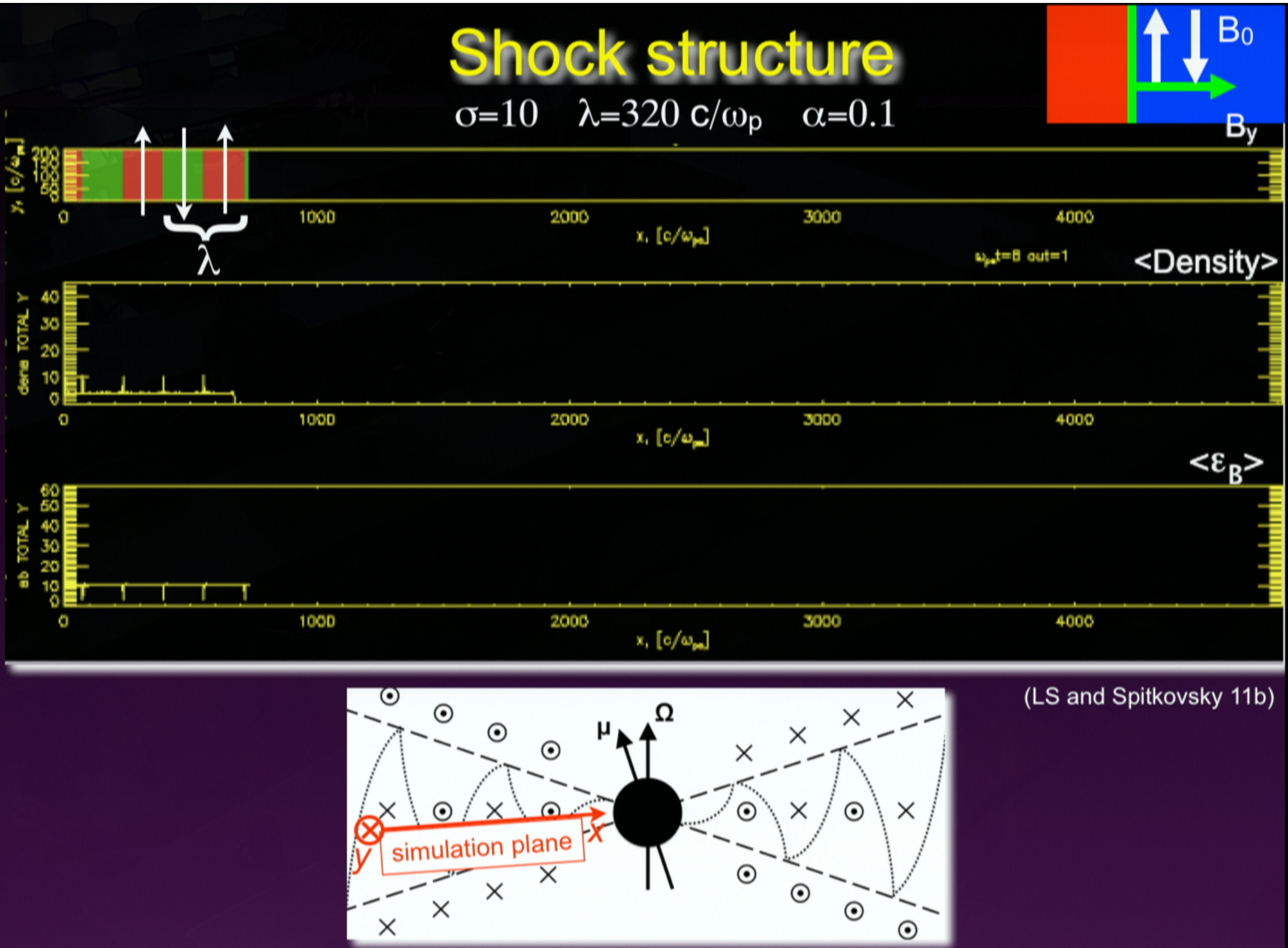


(LS and Spitkovsky 11b)

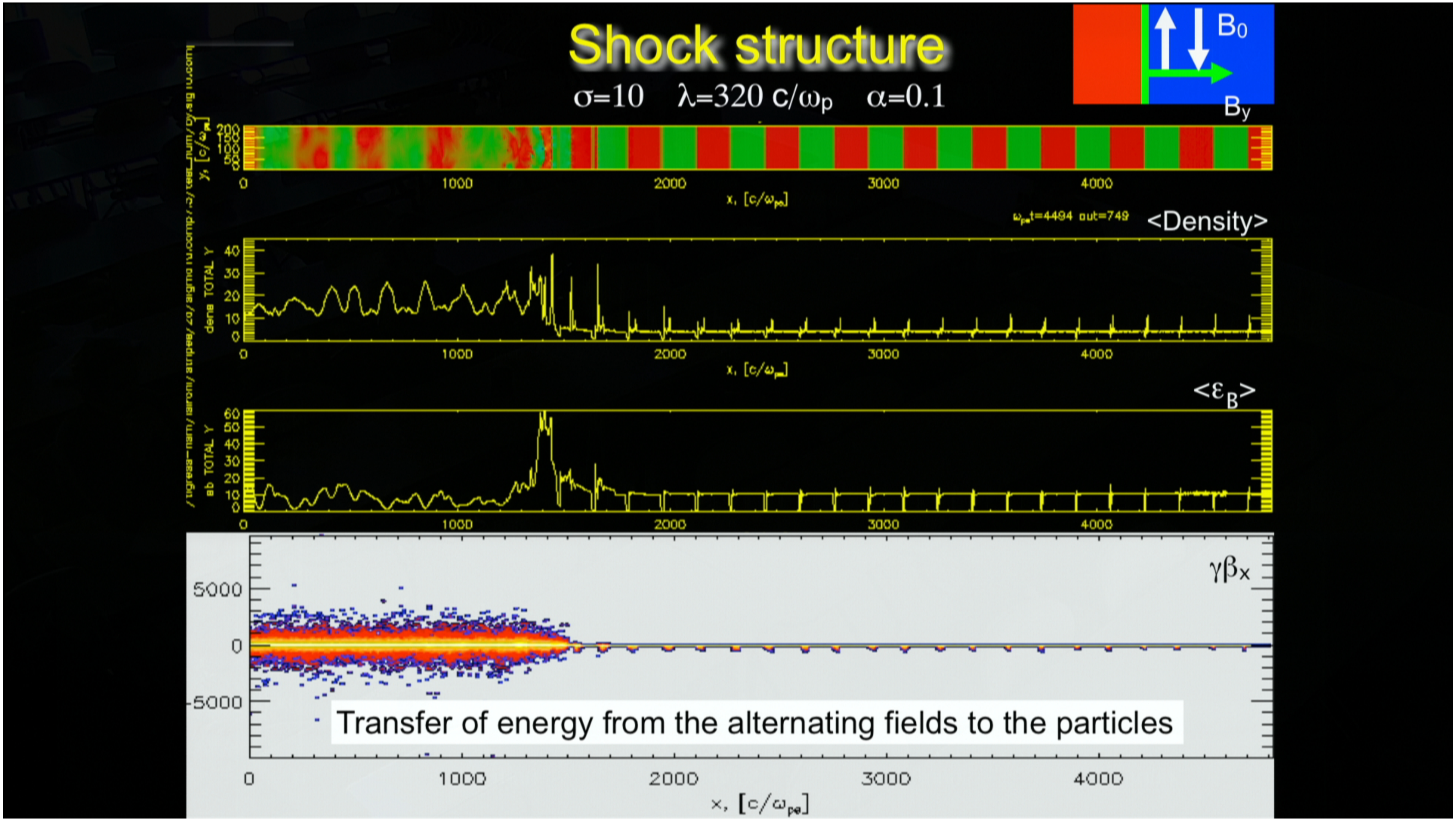
Shock structure
σ=10 λ=320 c/ωp α=0.1
B0
By
<Density>
<εB>
γβx
Transfer of energy from the alternating fields to the particles
x, [c/ωpe]

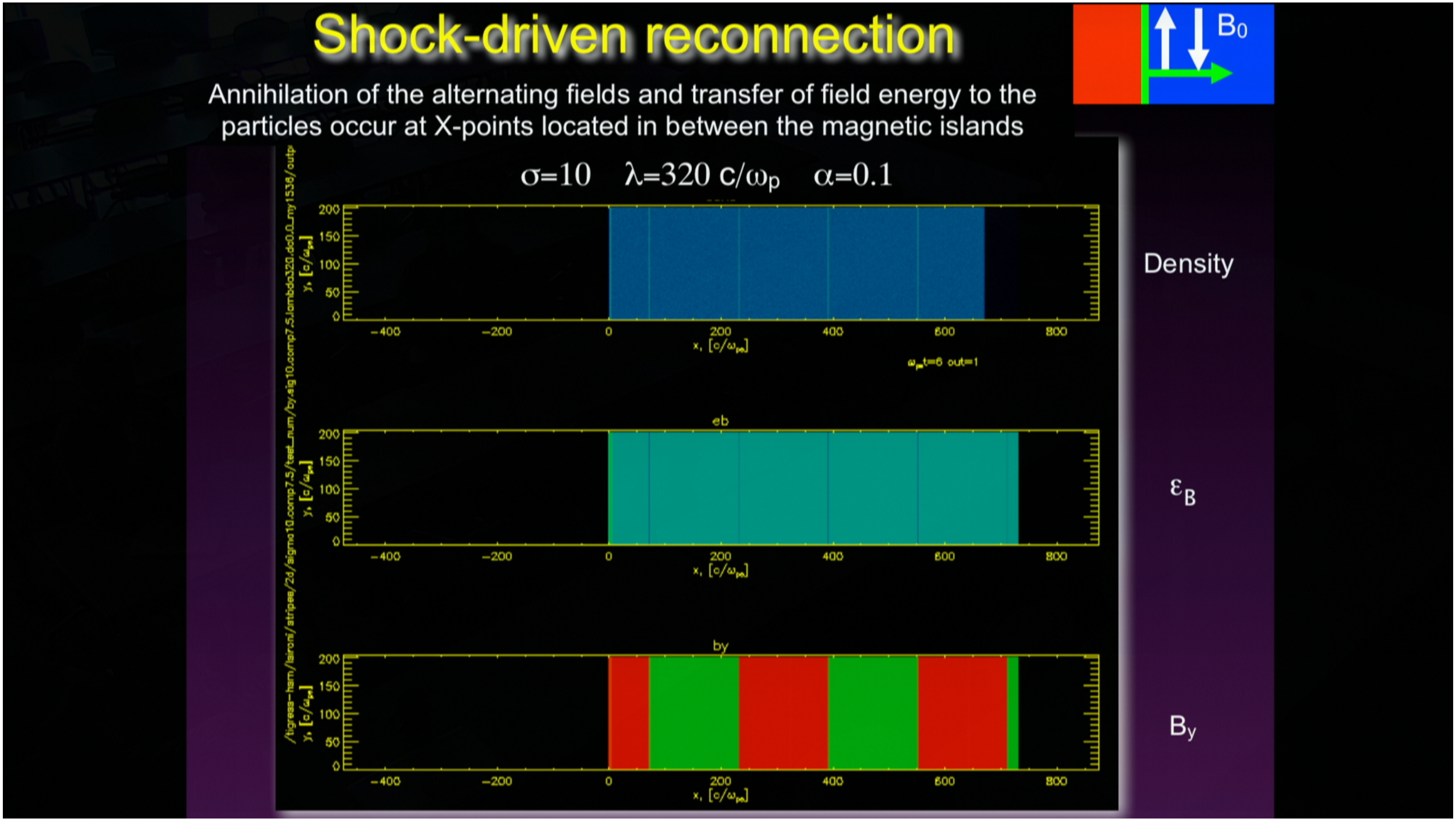

Shock-driven reconnection
Annihilation of the alternating fields and transfer of field energy to the particles occur at X-points located in between the magnetic islands
B0
σ=10 λ=320 c/ωp α=0.1
Density
εB
By
eb
by

# Shock-driven reconnection

σ=10 λ=640 c/ω$_p$ α=0.1

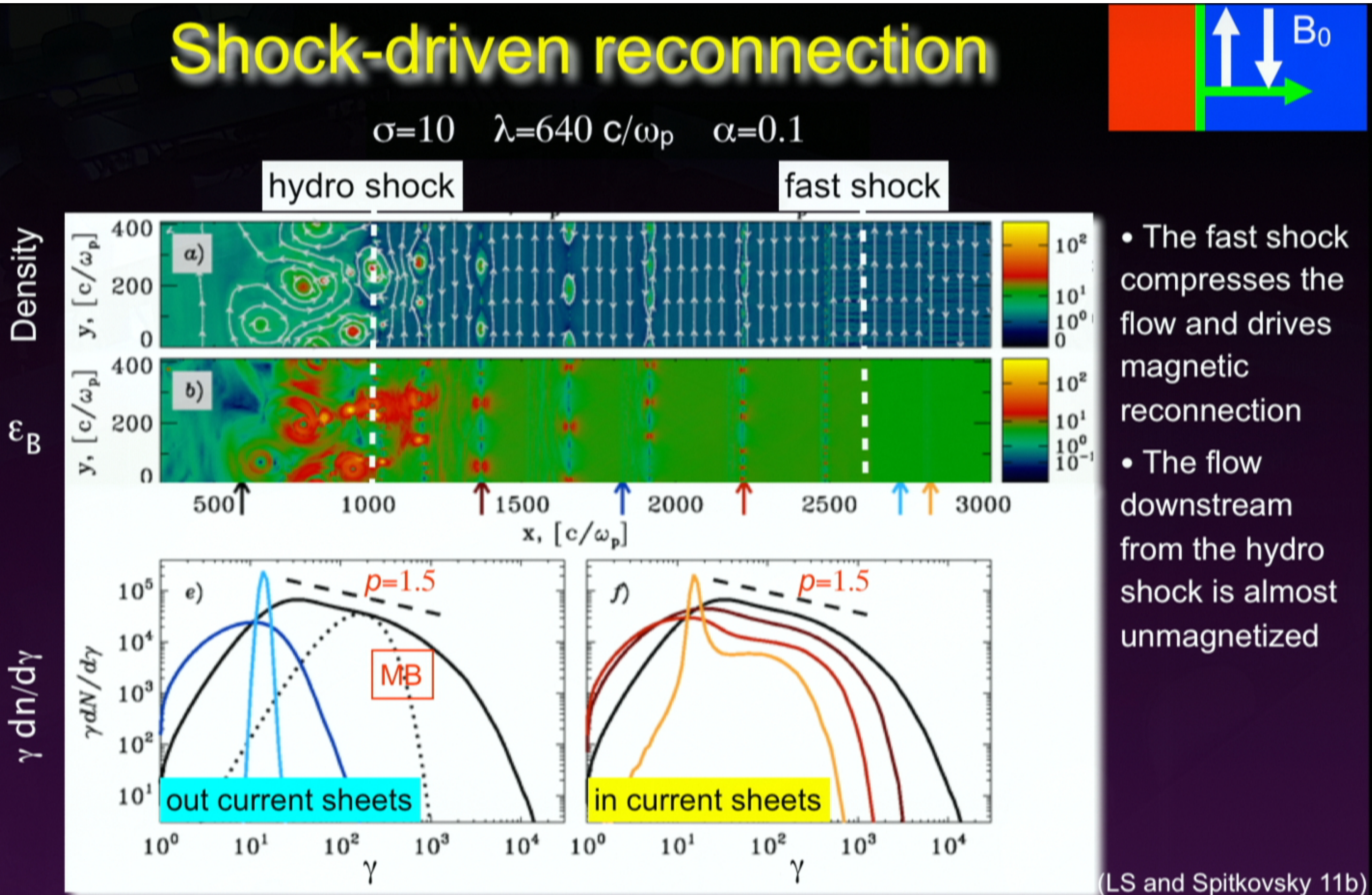


- The fast shock compresses the flow and drives magnetic reconnection
- The flow downstream from the hydro shock is almost unmagnetized

(LS and Spitkovsky 11b)

- The particle spectrum within current sheets gets broader from the fast to the hydro shock
- Behind the hydro shock, broad spectrum with flat tail of slope $p$~1.5

# Particle acceleration mechanism

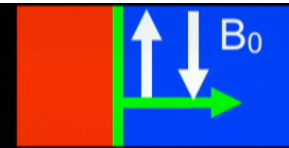


$\sigma=10 \quad \lambda=320\ c/\omega_p \quad \alpha=0.1$

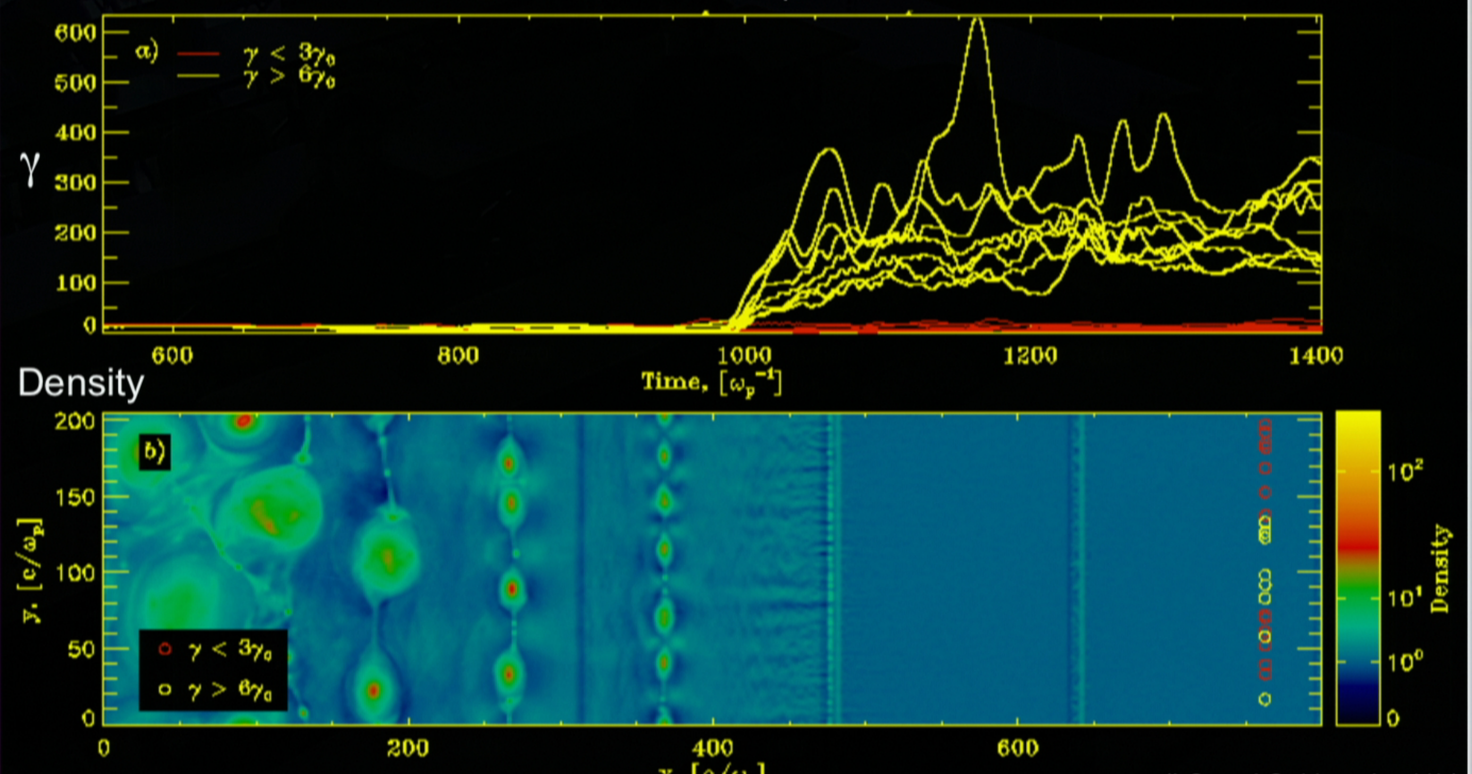


(LS and Spitkovsky 11b)

Particles are accelerated by the out-of-plane reconnection electric field at X-points. Acceleration proceeds until the particle is advected into the nearest island.

# Particle acceleration mechanism

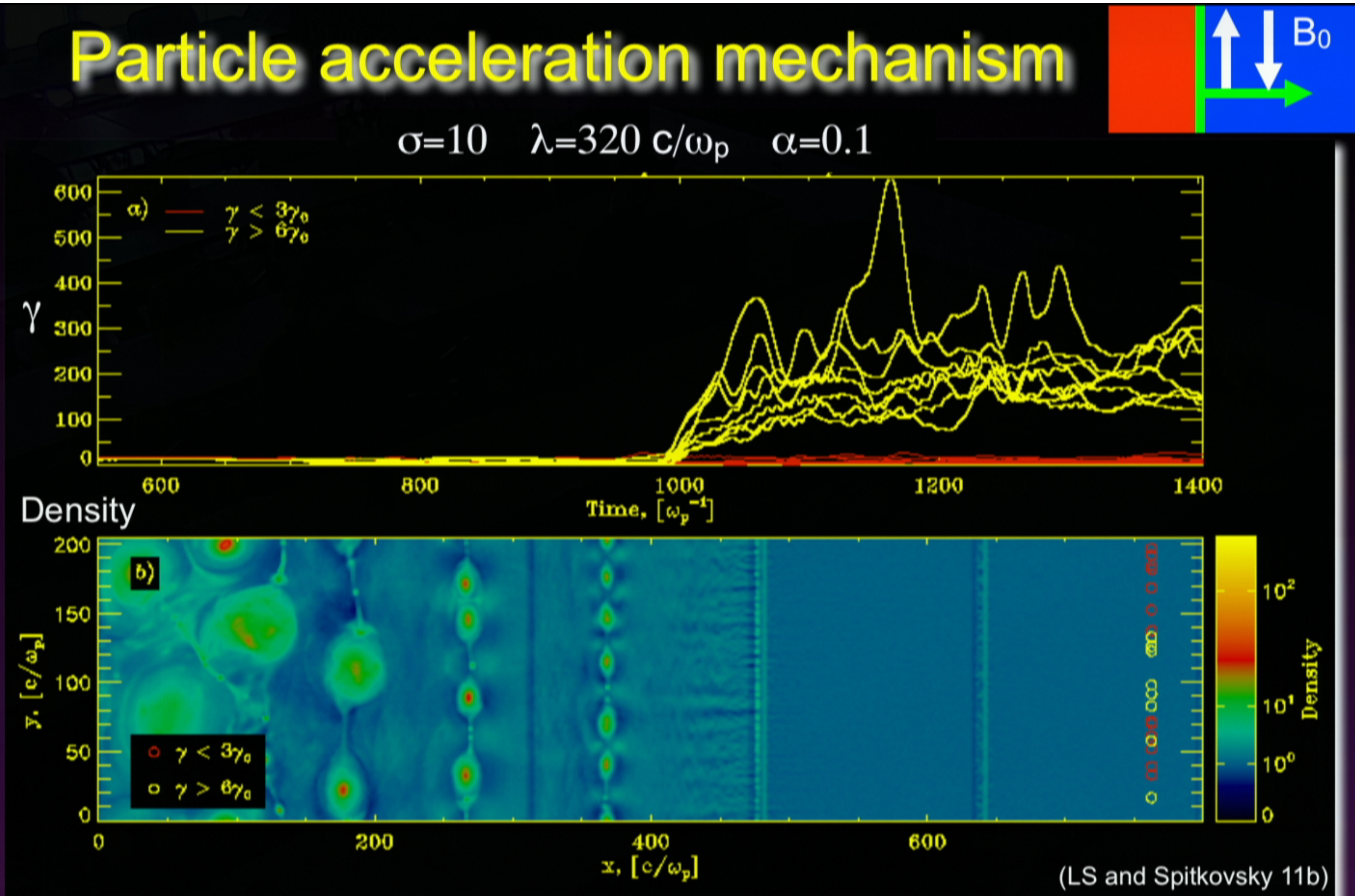


Particles are accelerated by the out-of-plane reconnection electric field at X-points. Acceleration proceeds until the particle is advected into the nearest island.

# Particle acceleration mechanism

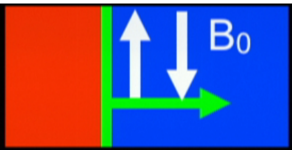


σ=10 λ=320 c/ωp α=0.1

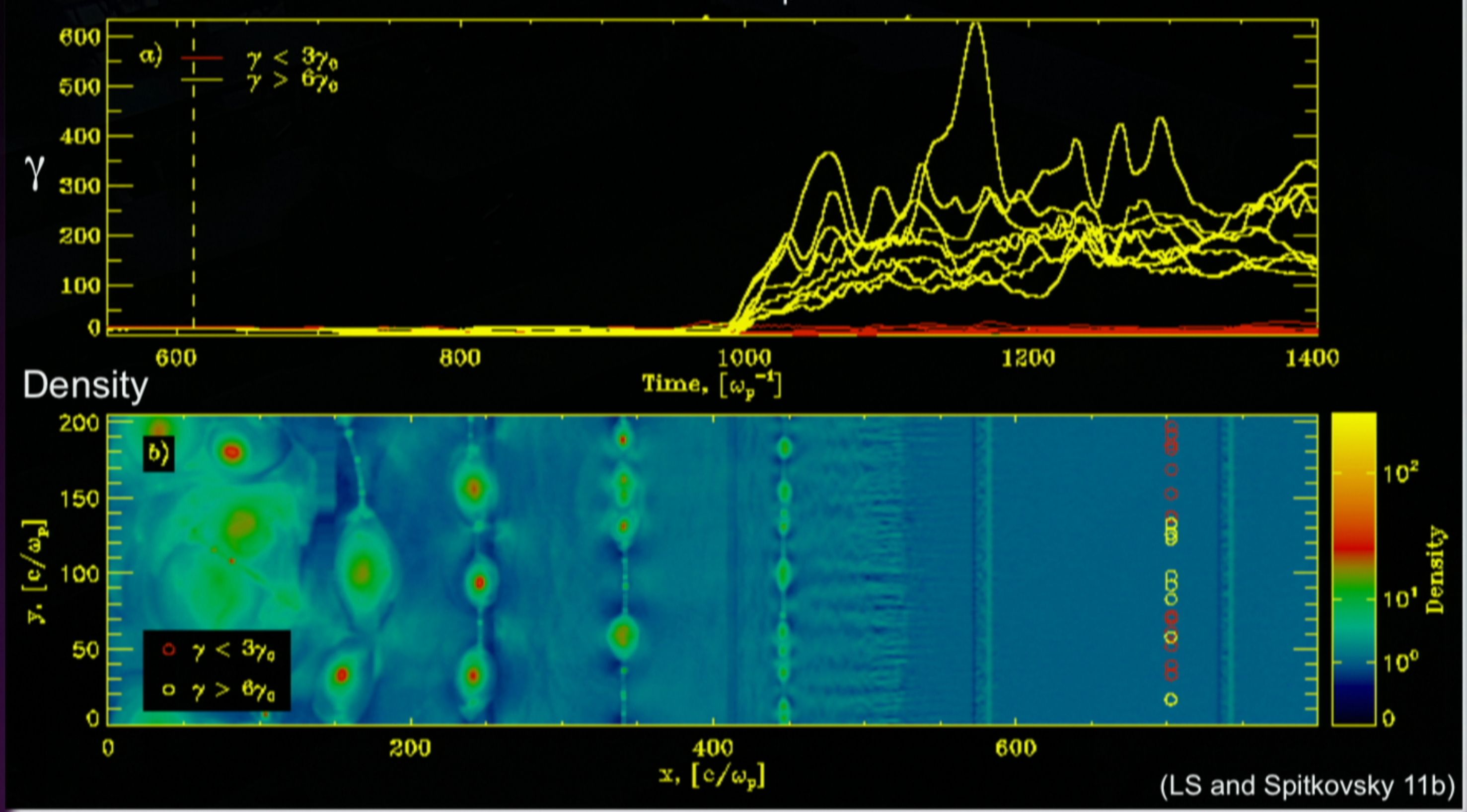


(LS and Spitkovsky 11b)

Particles are accelerated by the out-of-plane reconnection electric field at X-points.
Acceleration proceeds until the particle is advected into the nearest island.

# The particle energy spectrum

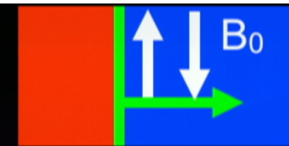


Varying the wavelength λ

Varying $\sigma = \frac{B_0^2}{4\pi\gamma_0 n_0 mc^2}$

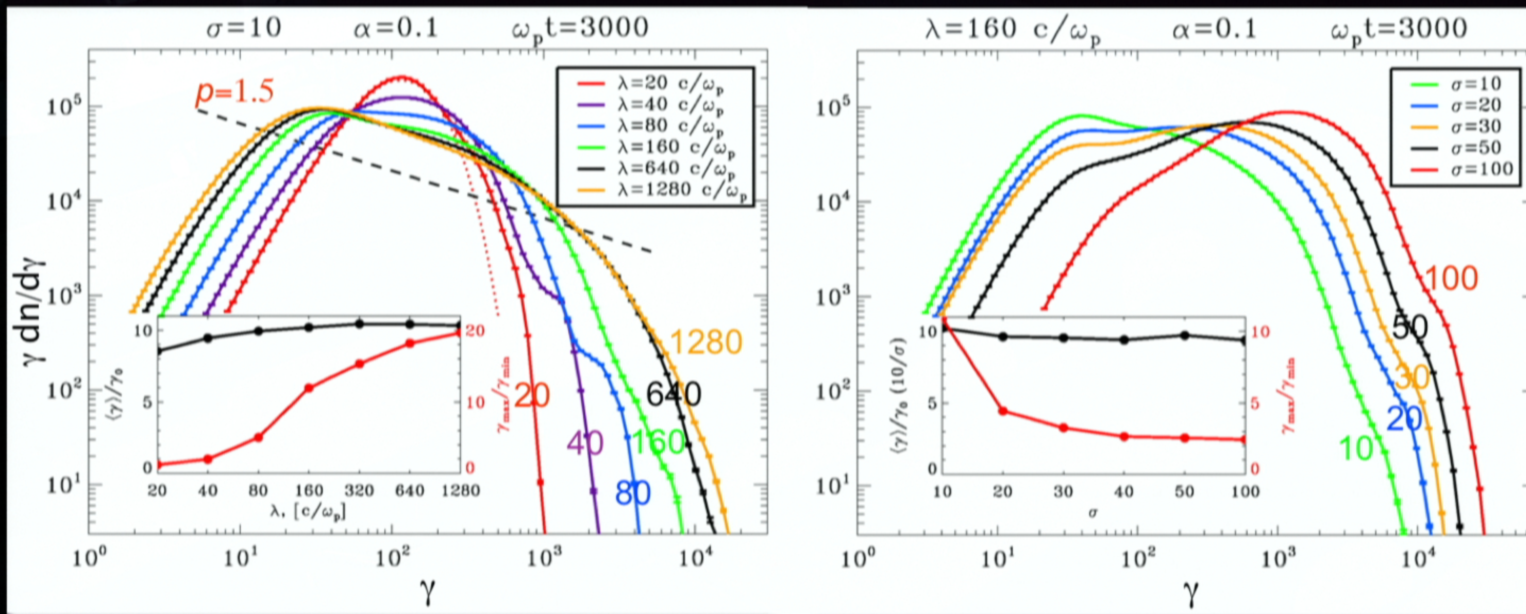


(LS and Spitkovsky 11b)

- Complete dissipation of the alternating fields for all λ and σ
- Average particle Lorentz factor grows across the shock from $\gamma_0$ up to $\gamma_0\,\sigma$
- With increasing λ or decreasing σ, the spectrum changes from a Maxwellian-like shape to a broad distribution with flat tail ($p\sim1.5$), with $\gamma_{min}\sim\gamma_0$ and $\gamma_{max}\sim\gamma_0\,\sigma^2$

# The particle energy spectrum

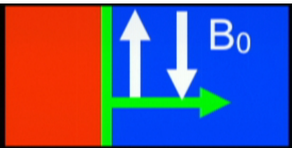


Varying the wavelength λ | Varying $\sigma = \frac{B_0^2}{4\pi\gamma_0 n_0 m c^2}$

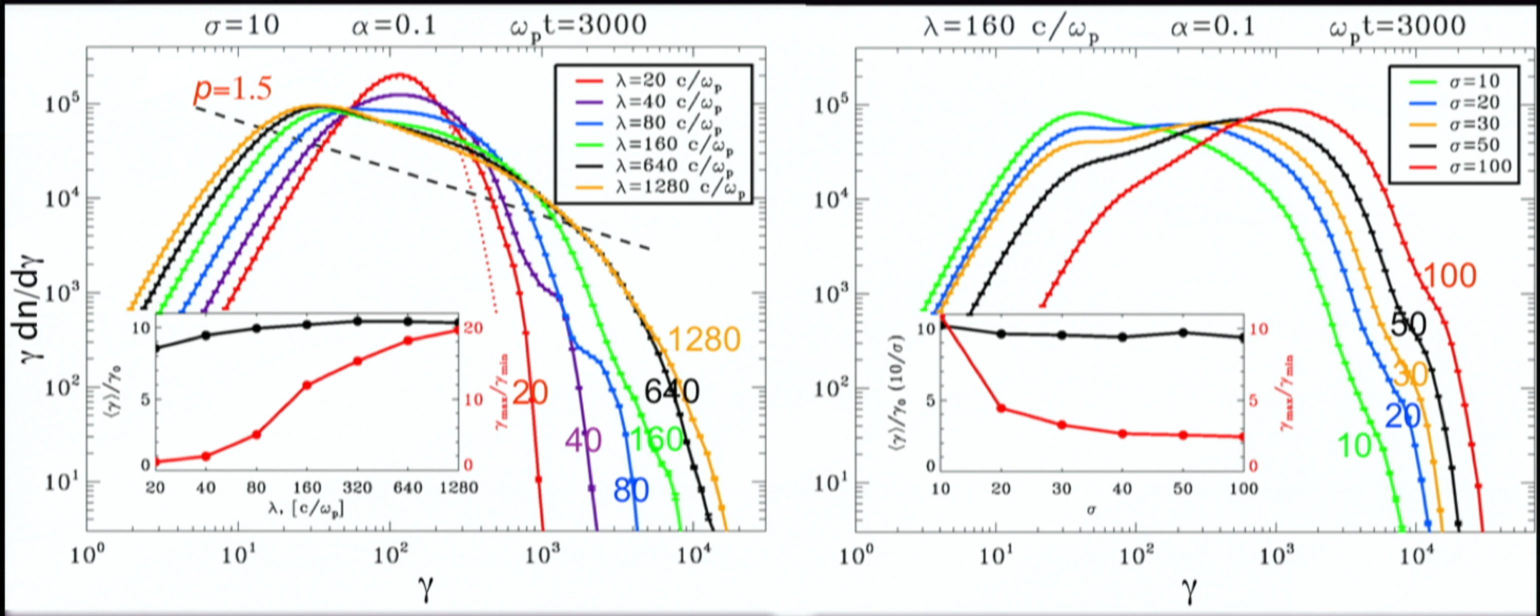


(LS and Spitkovsky 11b)

- Complete dissipation of the alternating fields for all λ and σ
- Average particle Lorentz factor grows across the shock from $\gamma_0$ up to $\gamma_0 \sigma$
- With increasing λ or decreasing σ, the spectrum changes from a Maxwellian-like shape to a broad distribution with flat tail ($p \sim 1.5$), with $\gamma_{min} \sim \gamma_0$ and $\gamma_{max} \sim \gamma_0 \sigma^2$

# The parameter $\lambda/r_L\sigma$

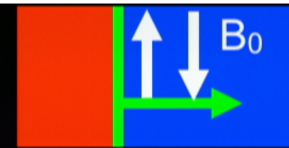


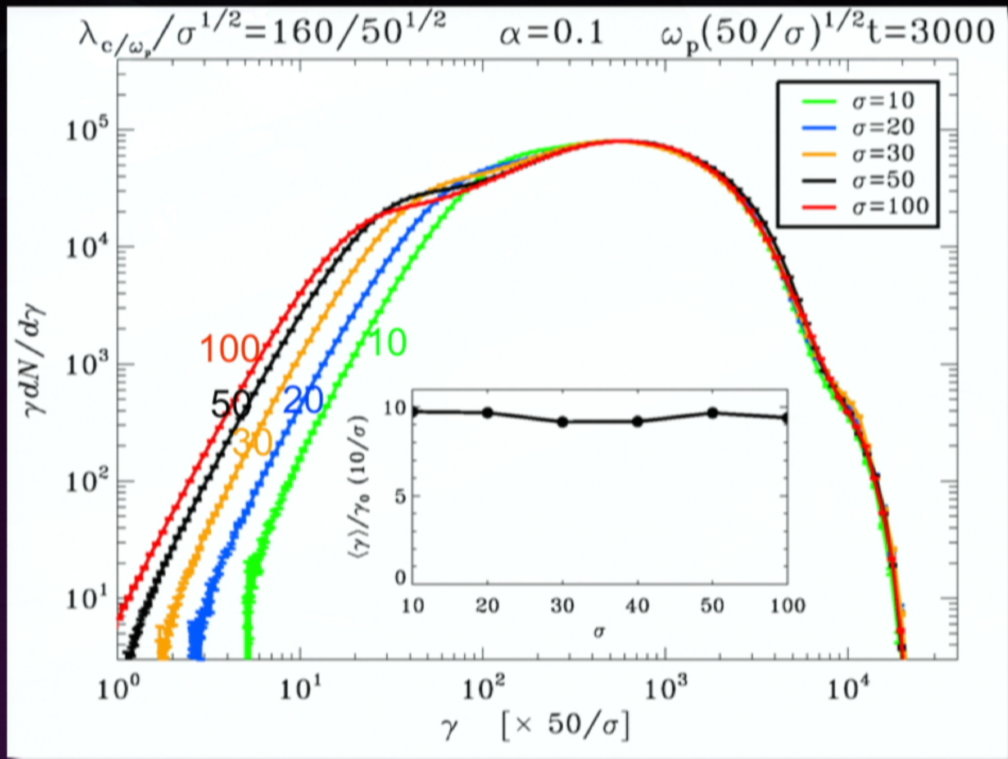


- We vary the wind magnetization and the stripe wavelength such that $\lambda/r_L\sigma$ is fixed ($r_L$ is the relativistic Larmor radius in the cold wind, $r_L= c/\omega_p/\sqrt{\sigma}$)
- Complete dissipation of alternating fields in all cases

(LS and Spitkovsky 11b)

The shape of the spectrum for $\sigma>>1$ is determined by the single parameter $\lambda/r_L\sigma$

$\lambda/r_L\sigma<10$: Maxwellian-like spectrum

$\lambda/r_L\sigma>10$: Broad flat power-law tail with $p$~1.5

# Dependence on the stripe-averaged field

We fix wavelength and magnetization, and change only $\langle B_y \rangle_\lambda$, or $\alpha = \frac{2\langle B_y\rangle_\lambda}{B_0 + |\langle B_y\rangle_\lambda|}$

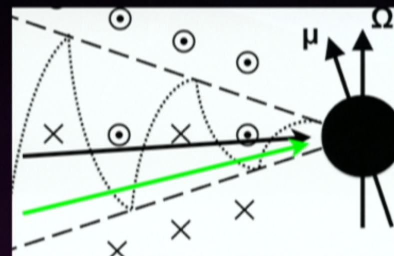


$\alpha$=0.1 (quasi-symmetric)

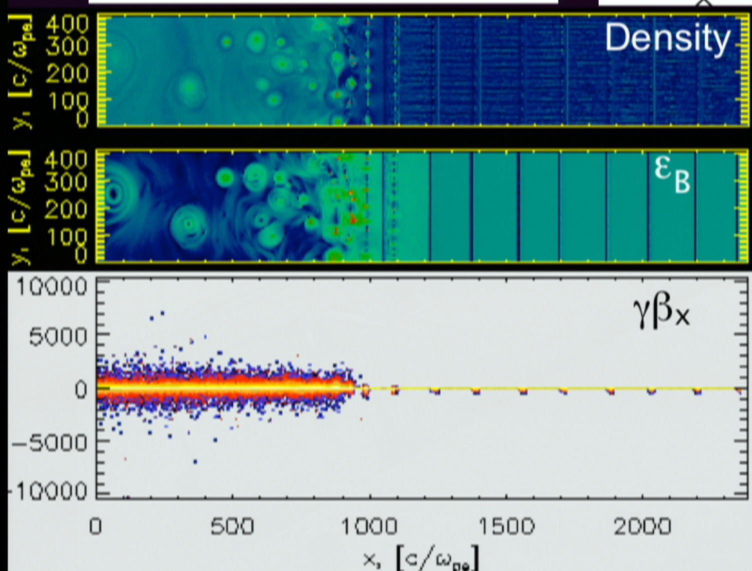


$\alpha$=0.75

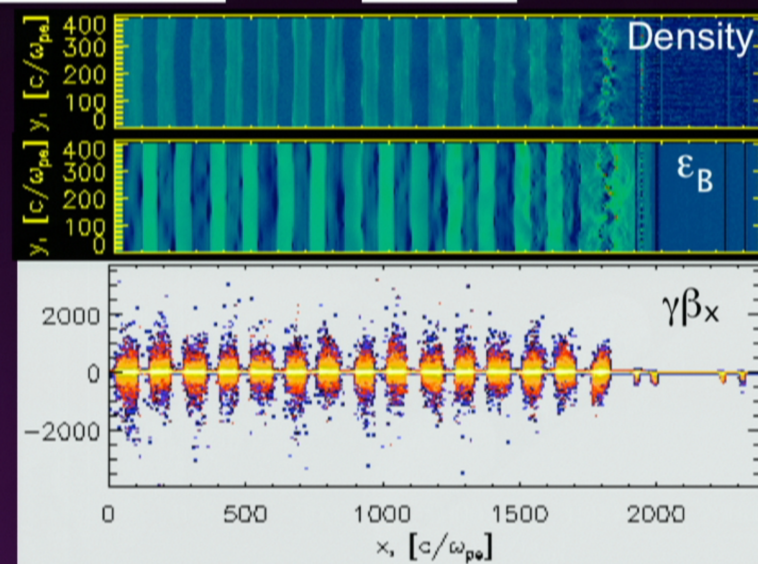


The alternating fields dissipate, the stripe-averaged field survives in regions of low-density cold plasma separated by sheets of hot particles

# Dependence on the stripe-averaged field

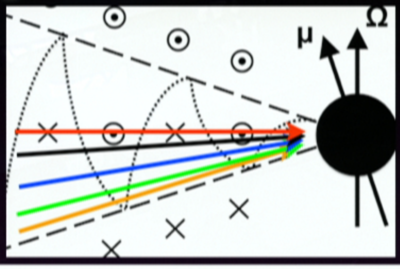


We explore the whole range of latitudes where the wind is striped (α from 0 to 1) $\alpha = \frac{2\langle B_y \rangle_\lambda}{B_0 + |\langle B_y \rangle_\lambda|}$

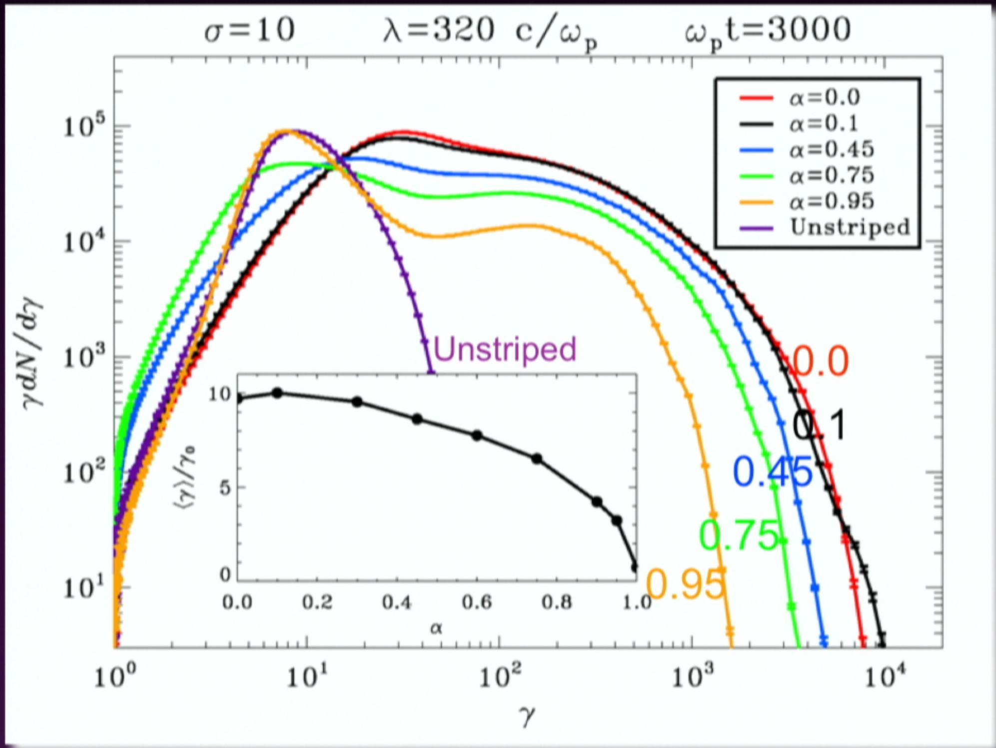


- With increasing α (i.e., away from the midplane), a smaller fraction of fields is in alternating form, and so available for dissipation
- The average particle Lorentz factor decreases from $\gamma_0 \sigma$ (for $\alpha=0$) down to $\gamma_0$ (for $\alpha \rightarrow 1$)
- The upper cutoff of the spectrum recedes with increasing α

# Dependence on the stripe-averaged field

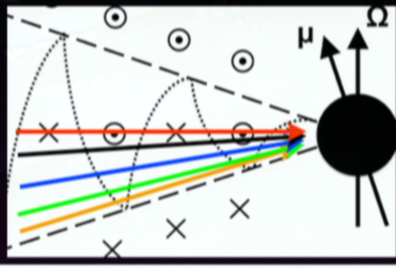


We explore the whole range of latitudes where the wind is striped (α from 0 to 1) $\alpha = \frac{2\langle B_y \rangle_\lambda}{B_0 + |\langle B_y \rangle_\lambda|}$

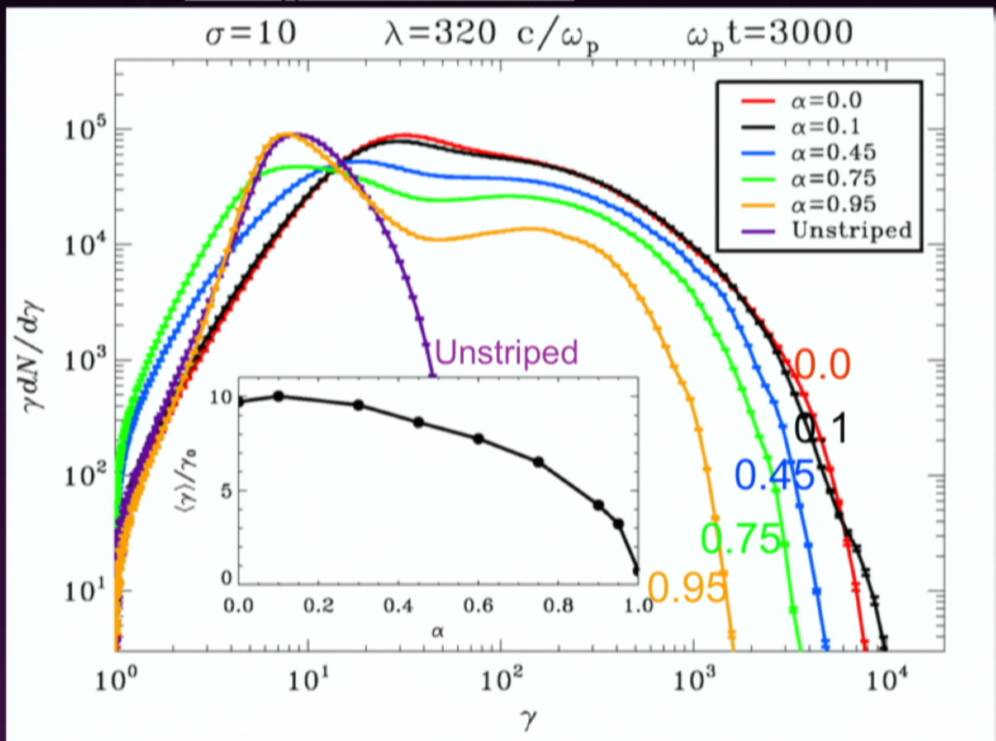


- With increasing α (i.e., away from the midplane), a smaller fraction of fields is in alternating form, and so available for dissipation
- The average particle Lorentz factor decreases from $\gamma_0 \sigma$ (for $\alpha=0$) down to $\gamma_0$ (for $\alpha \to 1$)
- The upper cutoff of the spectrum recedes with increasing α

# Dependence on the stripe-averaged field

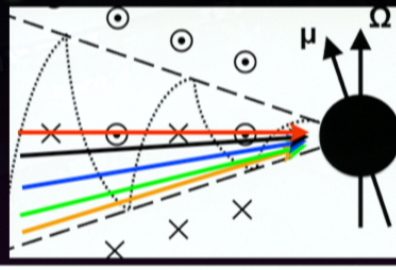


We explore the whole range of latitudes where the wind is striped ($\alpha$ from 0 to 1) $\alpha = \dfrac{2\langle B_y\rangle_\lambda}{B_0 + |\langle B_y\rangle_\lambda|}$

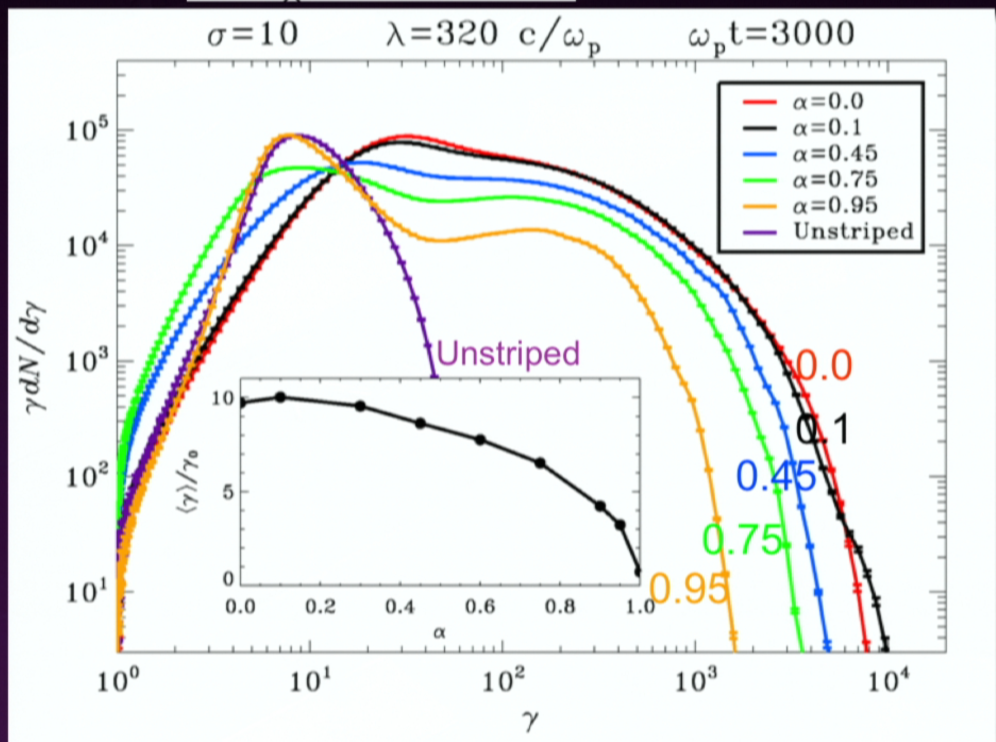


- With increasing $\alpha$ (i.e., away from the midplane), a smaller fraction of fields is in alternating form, and so available for dissipation
- The average particle Lorentz factor decreases from $\gamma_0\,\sigma$ (for $\alpha=0$) down to $\gamma_0$ (for $\alpha\to1$)
- The upper cutoff of the spectrum recedes with increasing $\alpha$

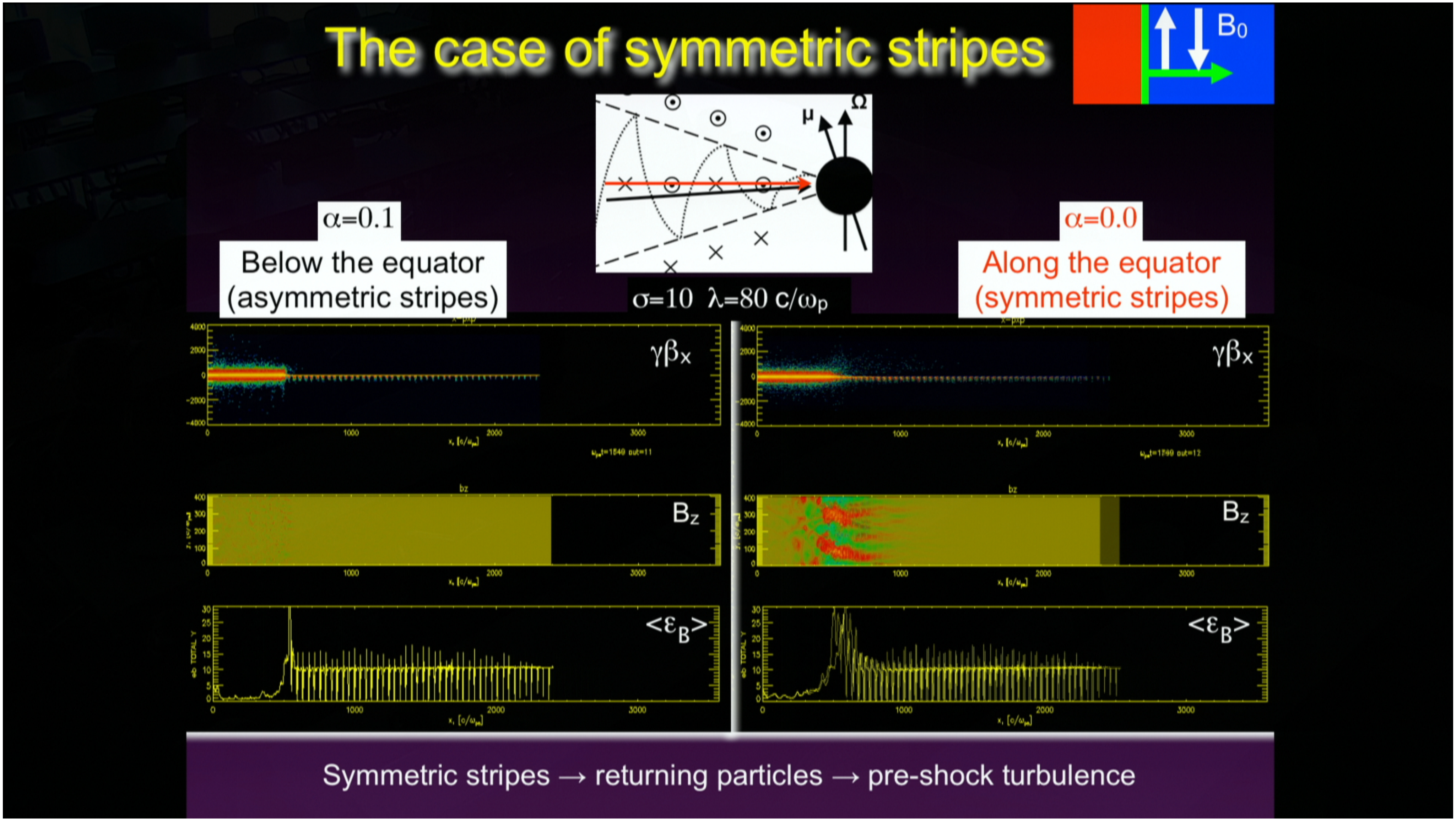
The case of symmetric stripes
$B_0$
μ
Ω
α=0.1
Below the equator
(asymmetric stripes)
σ=10 λ=80 c/ω$_p$
α=0.0
Along the equator
(symmetric stripes)
γβx
Bz
<εB>
Symmetric stripes → returning particles → pre-shock turbulence

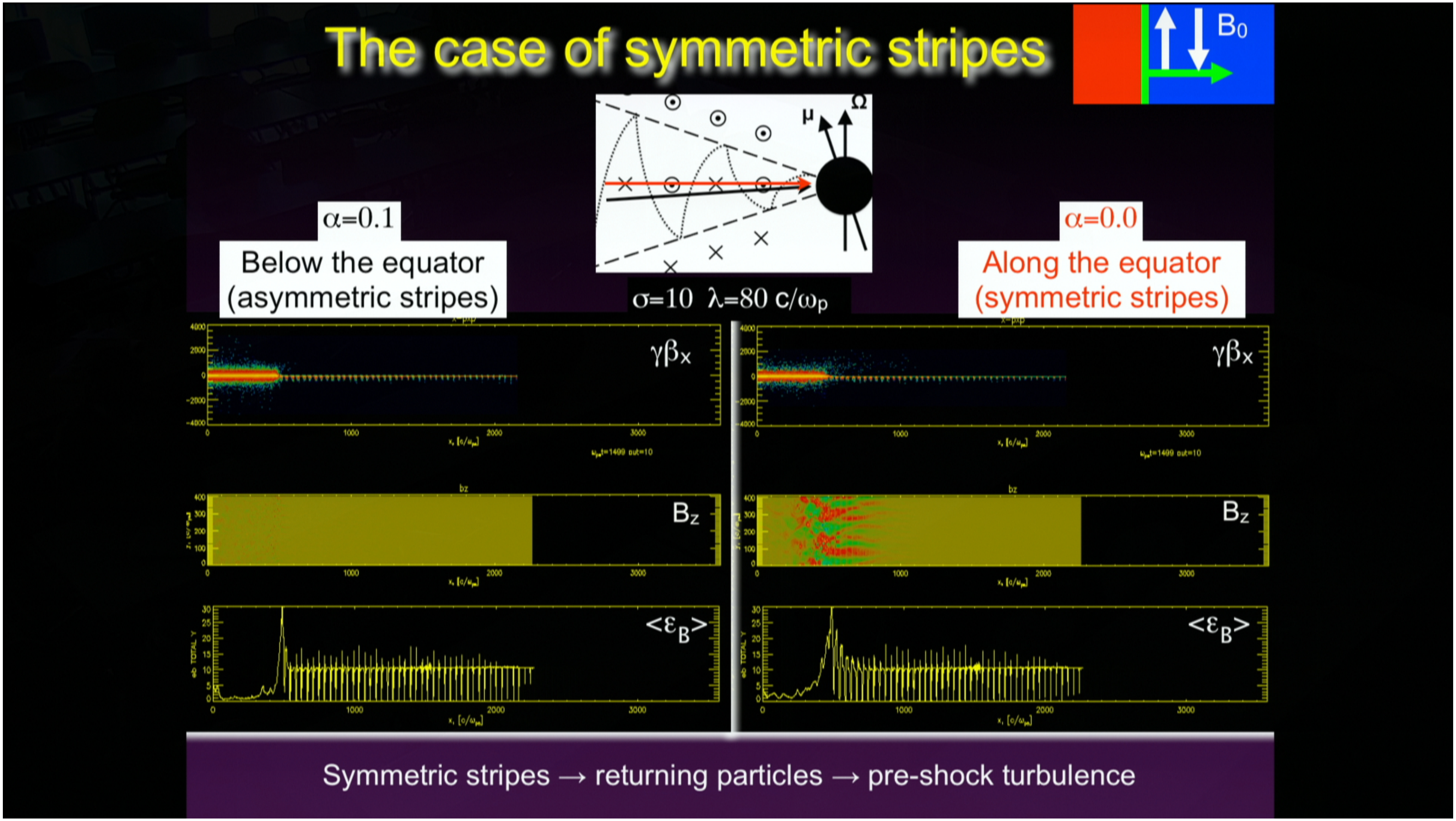
The case of symmetric stripes
B0
μ
Ω
α=0.1
Below the equator
(asymmetric stripes)
σ=10 λ=80 c/ωp
α=0.0
Along the equator
(symmetric stripes)
γβx
Bz
<εB>
Symmetric stripes → returning particles → pre-shock turbulence

# The case of symmetric stripes

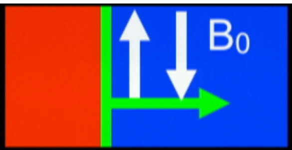


Symmetric stripes → returning particles → pre-shock turbulence

Pre-shock turbulence → Fermi-like diffusive acceleration

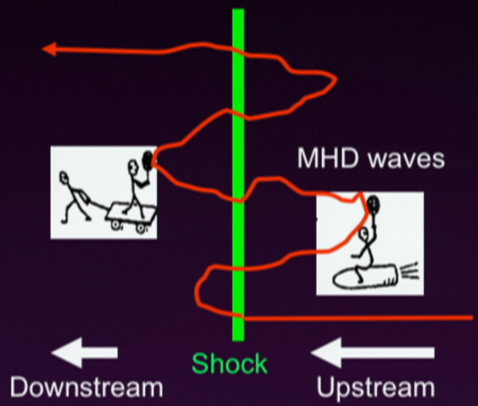

# The case of symmetric stripes

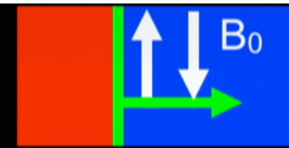


Symmetric stripes → returning particles → pre-shock turbulence

Pre-shock turbulence → Fermi-like diffusive acceleration

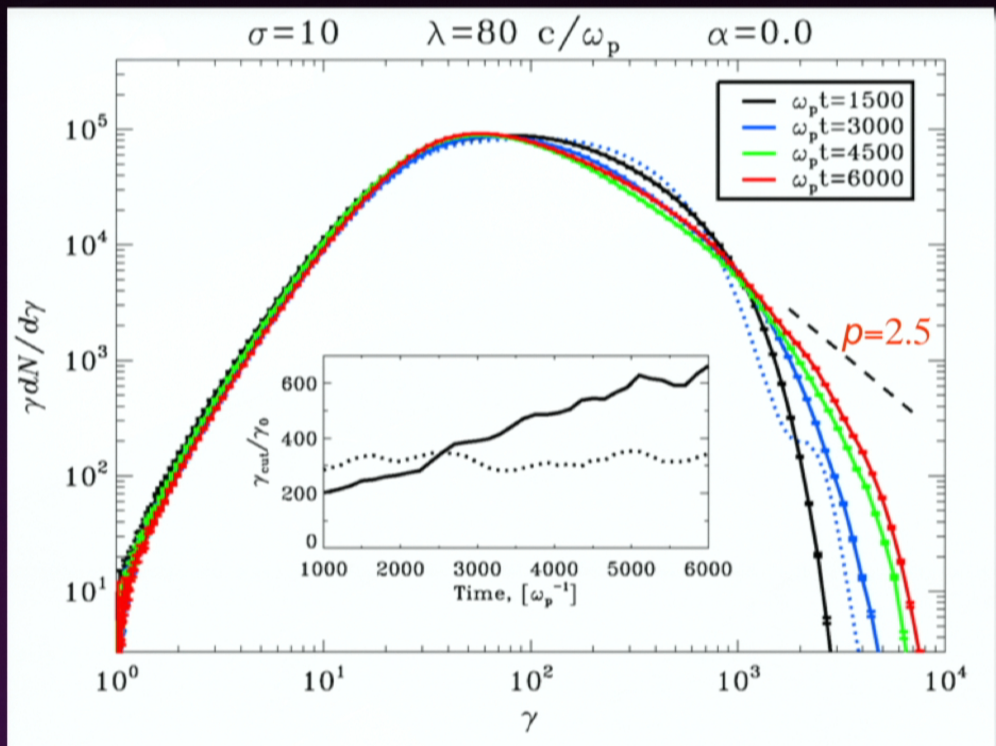


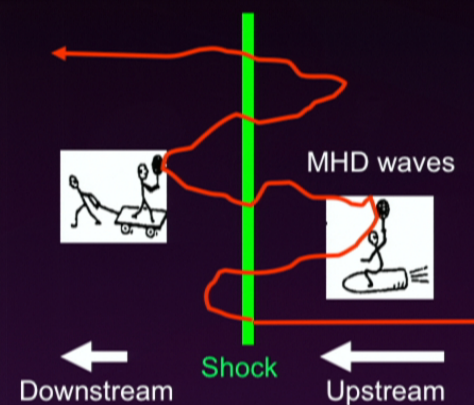


- Fermi-accelerated particles form a power-law tail of slope $p\sim2.5$
- The maximum Lorentz factor grows with time

(LS and Spitkovsky 11b)

# The case of symmetric stripes

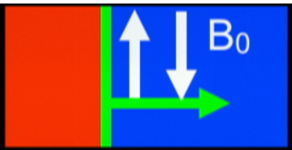


Symmetric stripes → returning particles → pre-shock turbulence

Pre-shock turbulence → Fermi-like diffusive acceleration

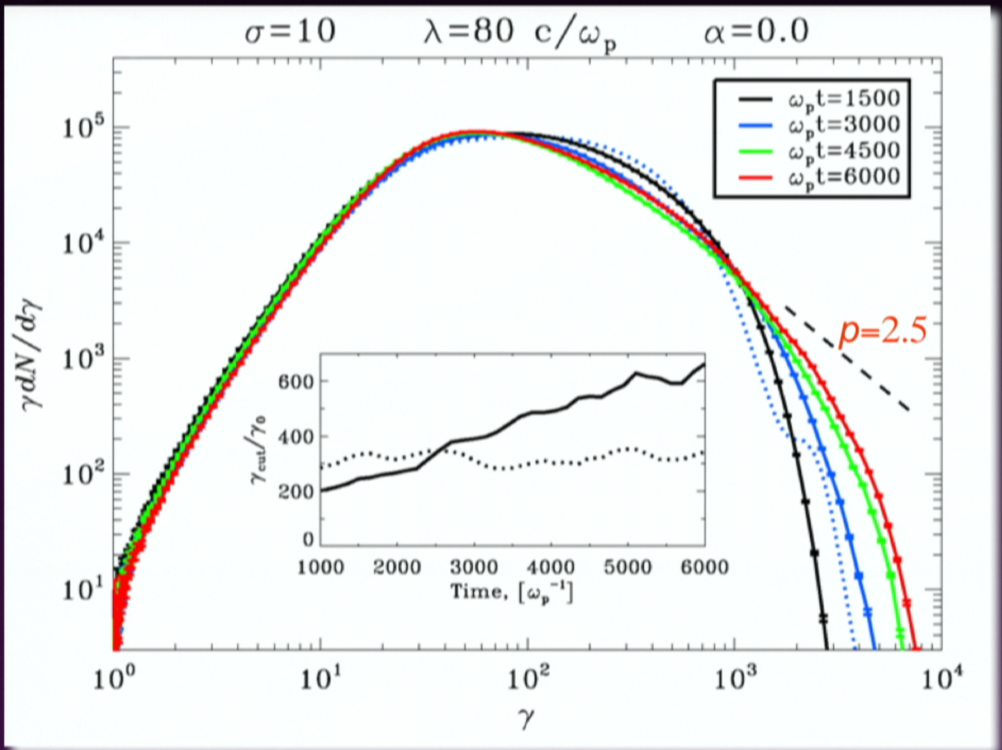


(LS and Spitkovsky 11b)

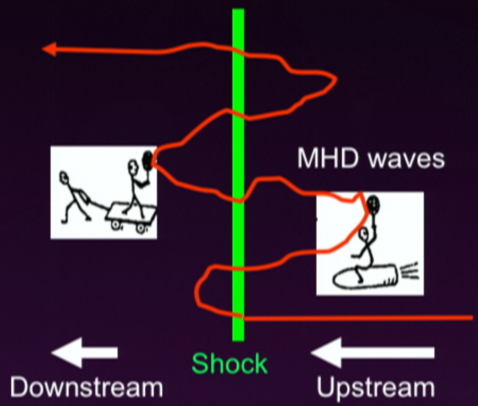


- Fermi-accelerated particles form a power-law tail of slope $p$~2.5
- The maximum Lorentz factor grows with time

# Dimensionality

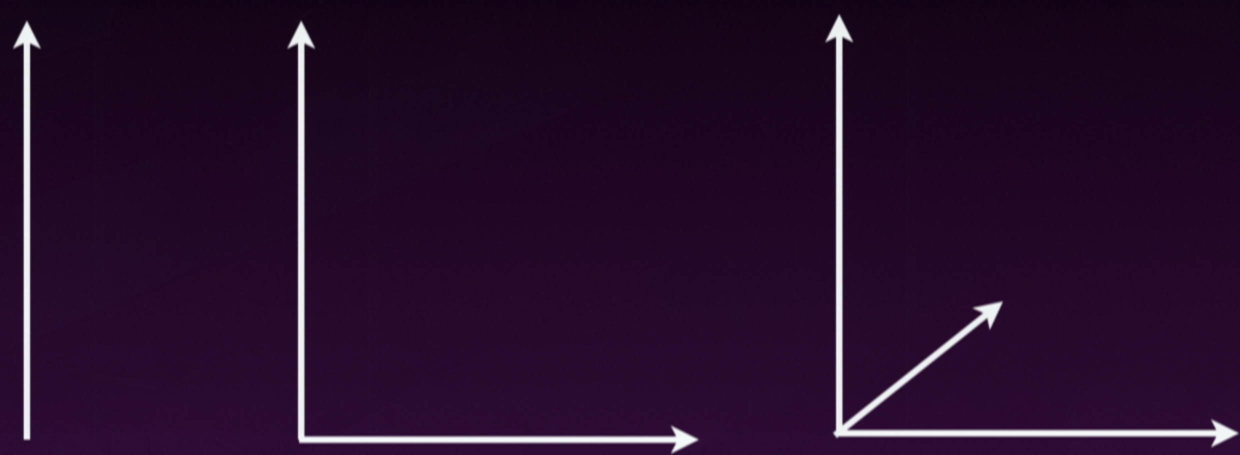

# 2D vs 1D

1D models cannot capture self-consistently the development of the tearing mode

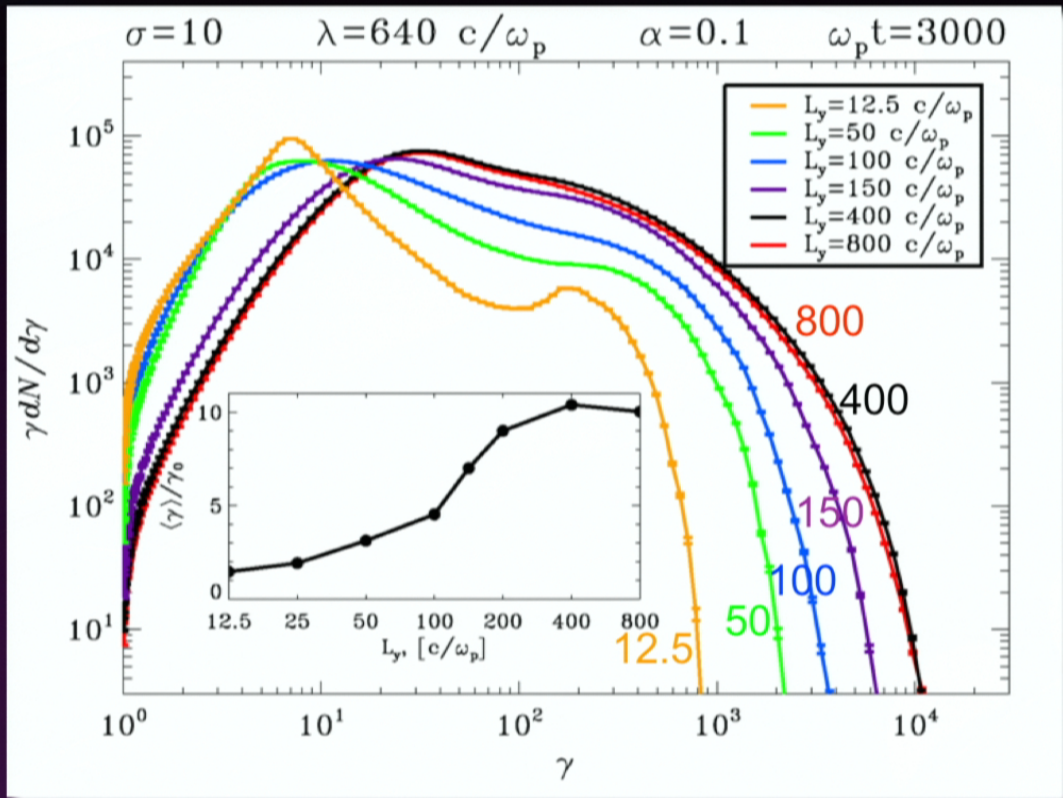


By reducing the transverse size of the box, we recover the results of the 1D model by Petri & Lyubarsky 2007

# 2D vs 1D

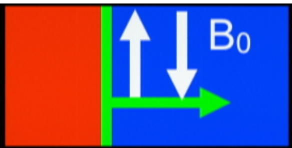


1D models cannot capture self-consistently the development of the tearing mode

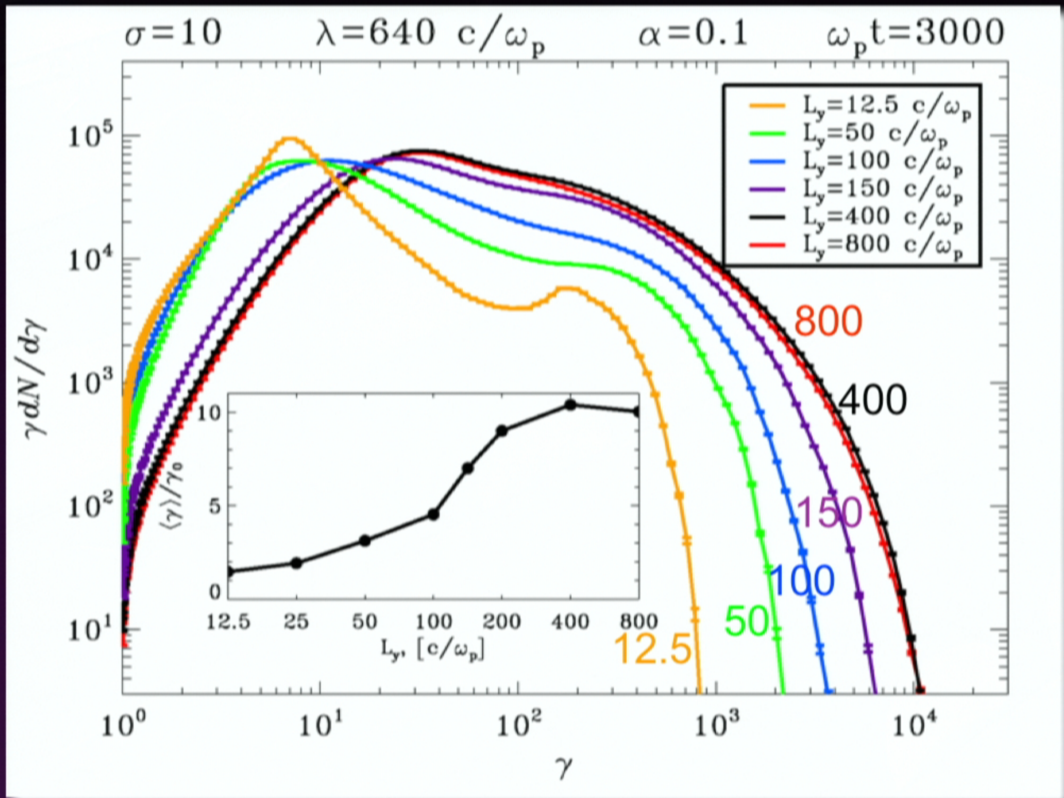


By reducing the transverse size of the box, we recover the results of the 1D model by Petri & Lyubarsky 2007

# 2D vs 3D: shock structure

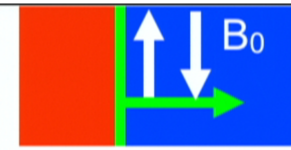


$\sigma=10 \quad \lambda=160\ c/\omega_p \quad \alpha=0.1$

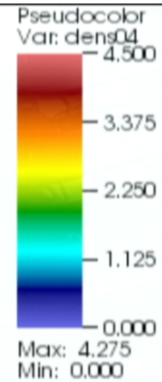


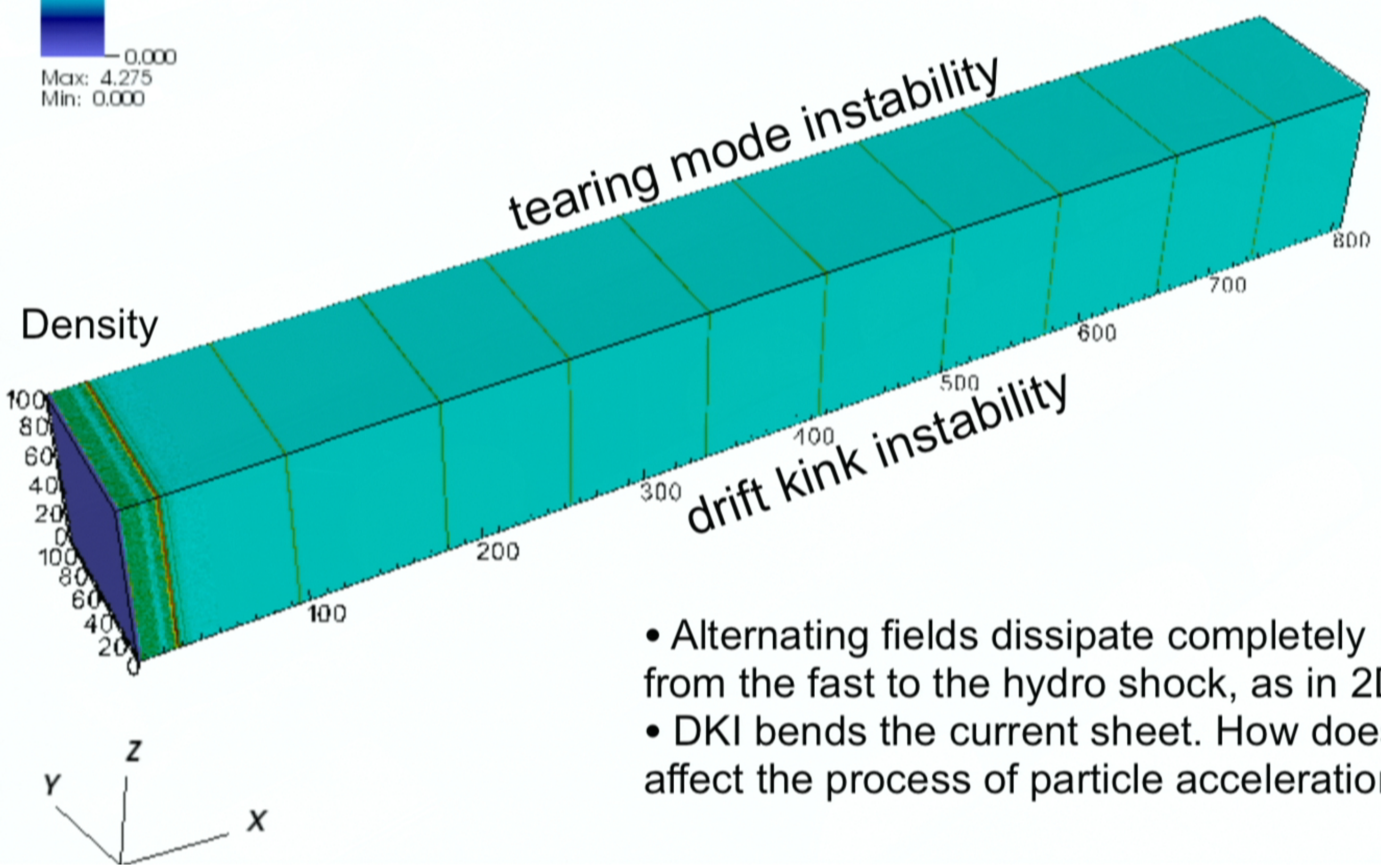


- Alternating fields dissipate completely from the fast to the hydro shock, as in 2D
- DKI bends the current sheet. How does it affect the process of particle acceleration?

# Implications for PWNe

- Particle acceleration via reconnection in a "striped" shock can give $p$~1.5, as required for the radio spectrum of the Crab Nebula. But a flat broad spectrum requires $\lambda/r_L\sigma>10$, whereas for the Crab (in the midplane) $$\frac{\lambda}{r_L\sigma} = 4\pi\kappa\frac{R_{LC}}{R_{TS}} \simeq 6\times10^{-8}\kappa$$

Alternatives:

✦ radio spectrum produced at high latitudes

✦ can $\kappa$ be as large as $10^8$, at least in the midplane?

- In the midplane, where the stripes are symmetric, particles pre-energized by the reconnection field can escape ahead of the shock, and be accelerated via a Fermi-like diffusive process. They may be responsible for the steep X-ray spectrum of the Crab (that requires $p$>2).

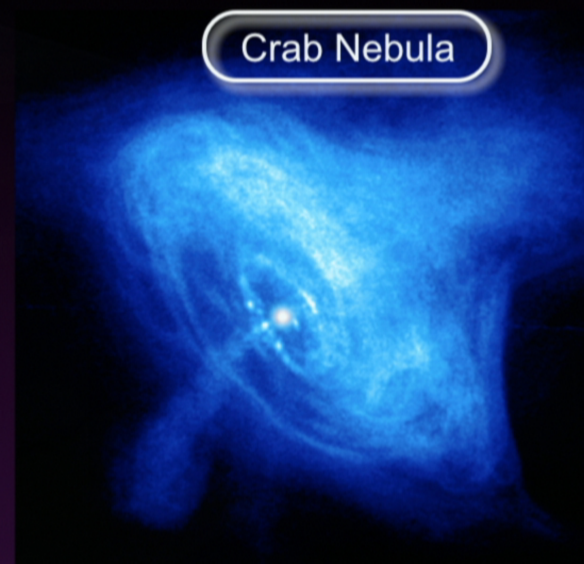


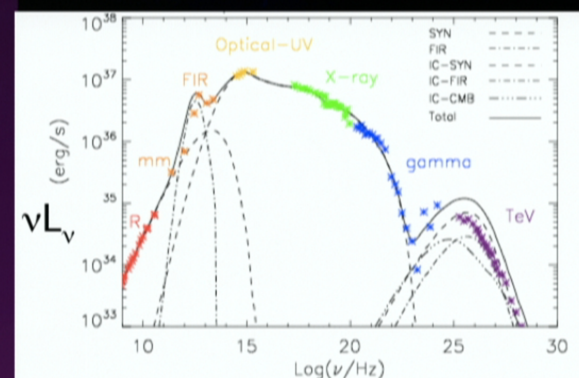

# Implications for PWNe

- Particle acceleration via reconnection in a "striped" shock can give $p\sim1.5$, as required for the radio spectrum of the Crab Nebula. But a flat broad spectrum requires $\lambda/r_L\sigma>10$, whereas for the Crab (in the midplane) $$\frac{\lambda}{r_L\sigma} = 4\pi\kappa\frac{R_{LC}}{R_{TS}} \simeq 6\times10^{-8}\kappa$$

Alternatives:

✦ radio spectrum produced at high latitudes

✦ can $\kappa$ be as large as $10^8$, at least in the midplane?

- In the midplane, where the stripes are symmetric, particles pre-energized by the reconnection field can escape ahead of the shock, and be accelerated via a Fermi-like diffusive process. They may be responsible for the steep X-ray spectrum of the Crab (that requires $p>2$).

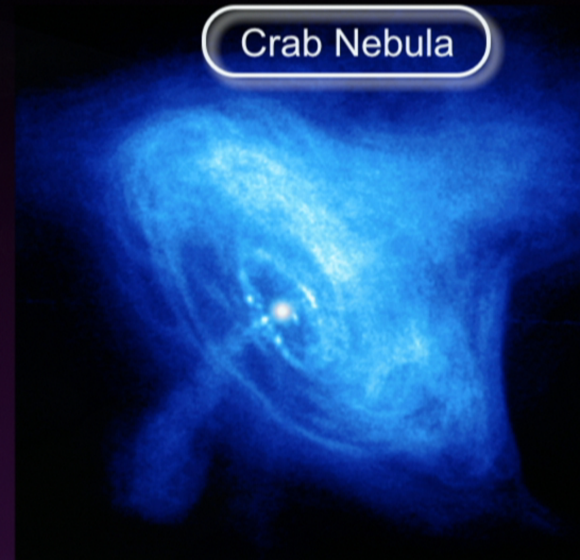


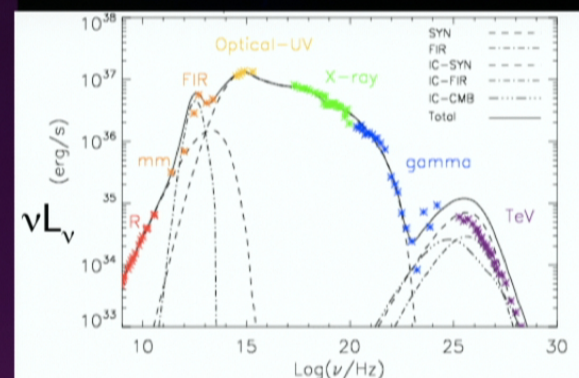

# Reconnection in pulsar winds & jets

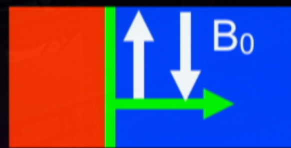


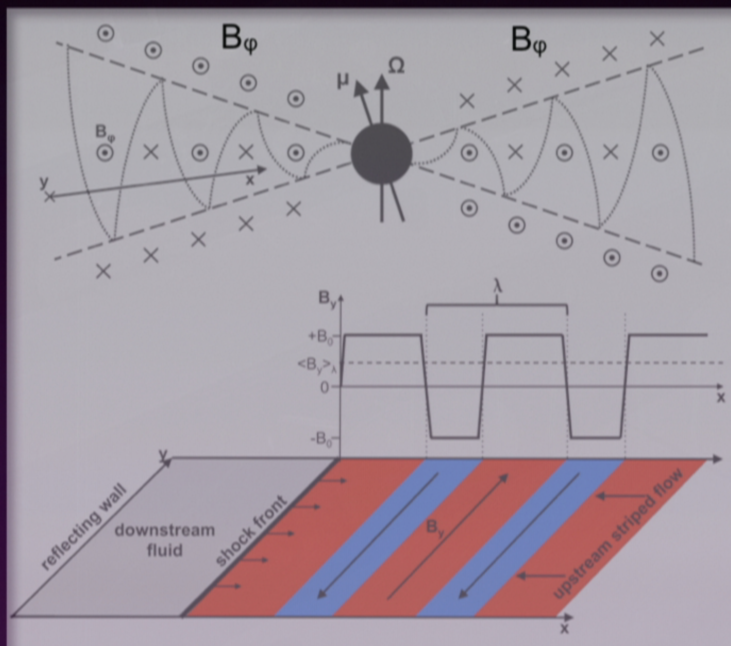


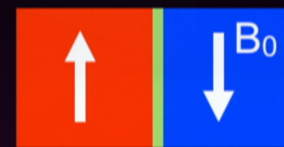


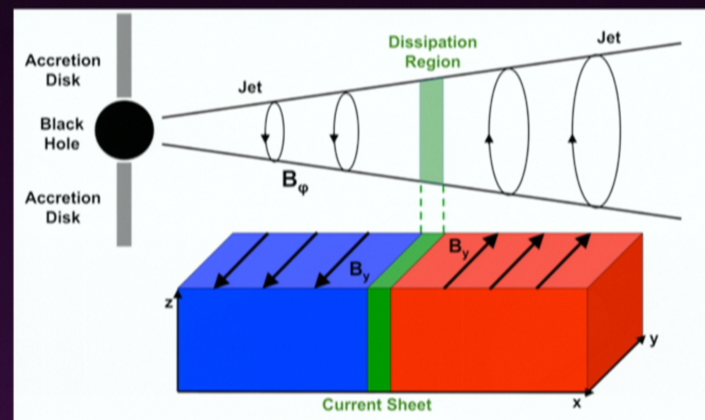


- A single dissipation region / current sheet
- No interaction with a shock

# A hierarchical process

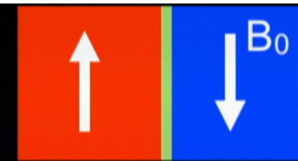


σ=10 electron-positron

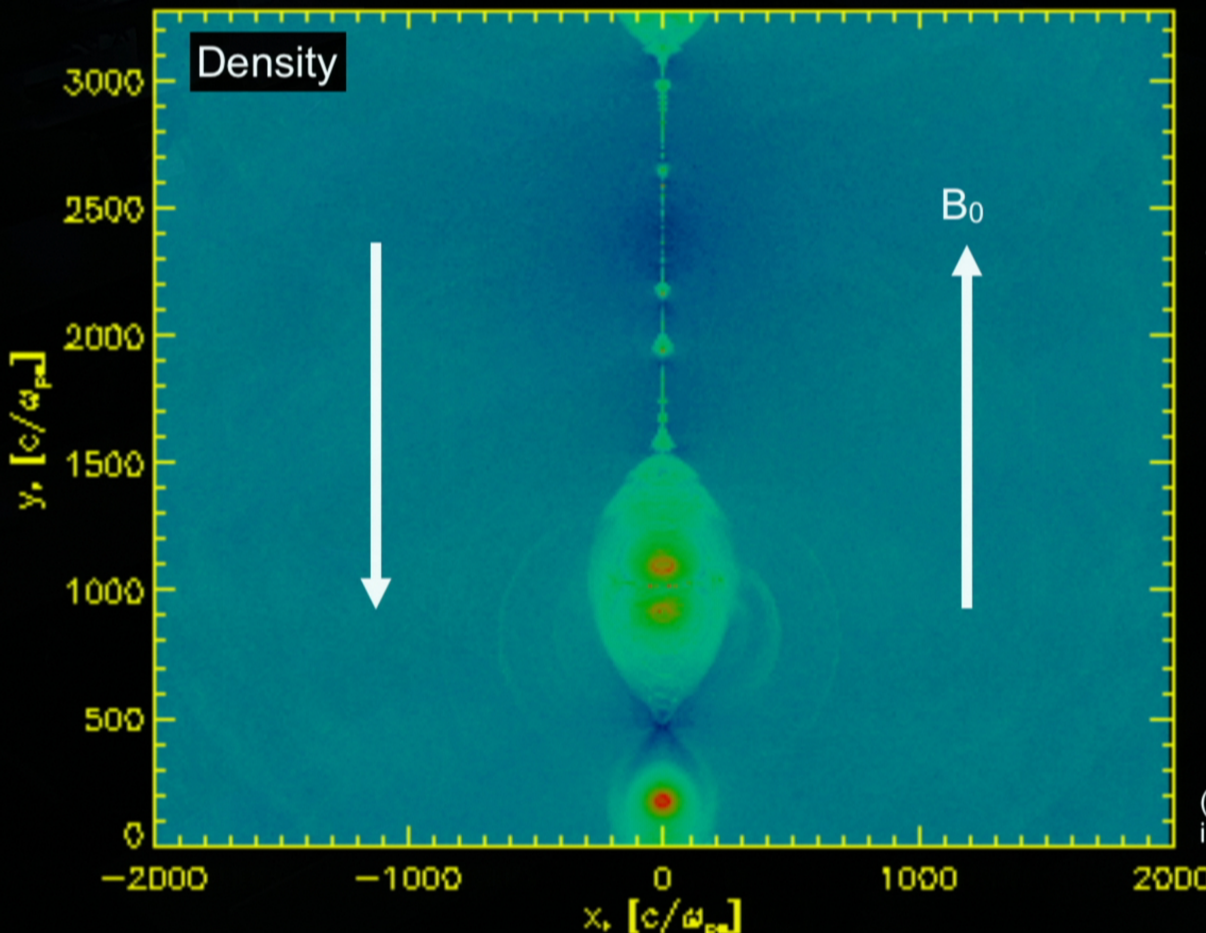


- Magnetic reconnection is a hierarchical process of island formation and merging.
- When two islands merge, an anti-reconnection layer is formed in between.

(LS 13, in prep)

# The particle spectrum

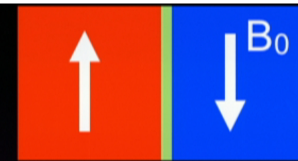


$\sigma$=10

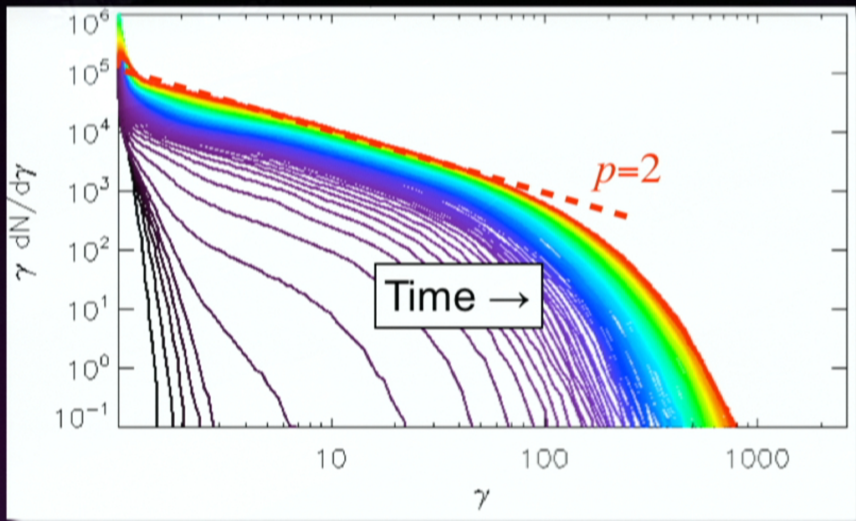


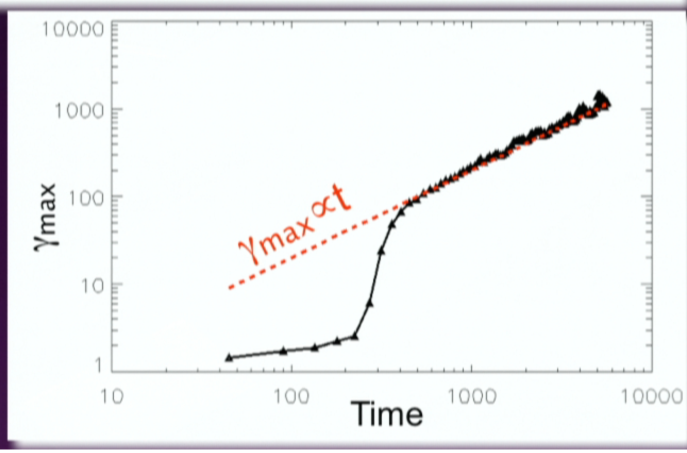


(LS 13, in prep)

- At late times, the particle spectrum in the current sheet approaches a power-law tail of slope *p*~2, extending in time to higher and higher energies.

- The maximum energy grows as $\gamma_{max} \propto t$ (as compared to $\gamma_{max} \propto t^{1/2}$ in shocks).

# Dependence on the magnetization

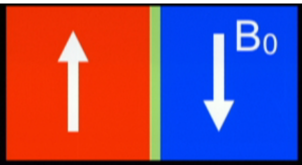


$$\sigma = \frac{B_0^2}{4\pi n_0 m_p c^2}$$

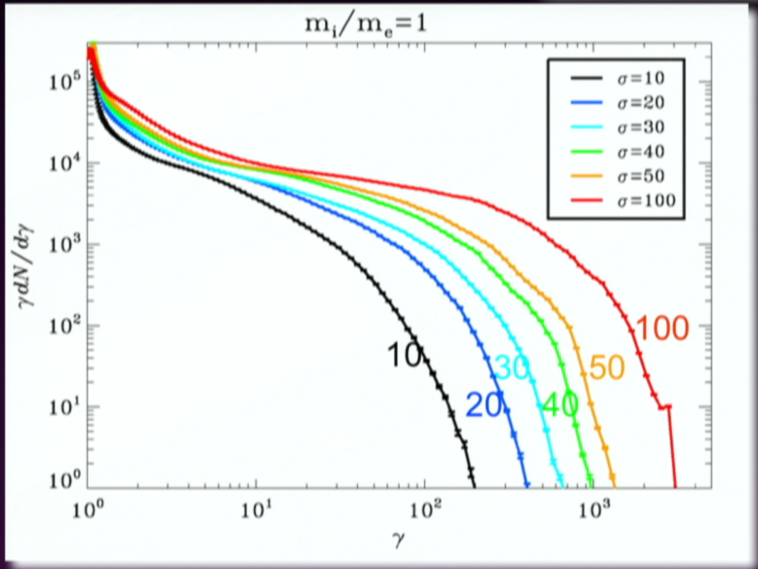

# 3D: fluid structure

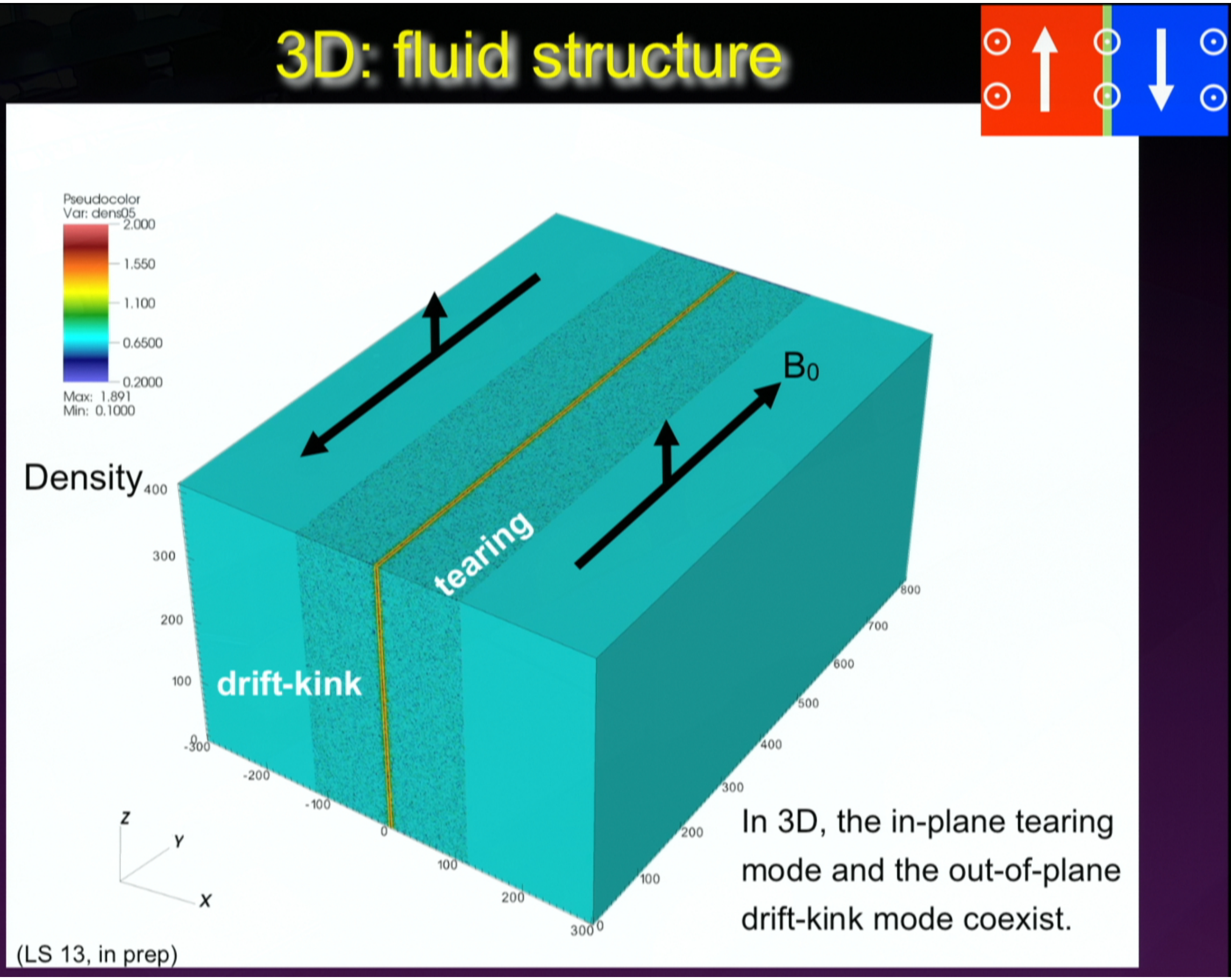

# Implications for AGN jets

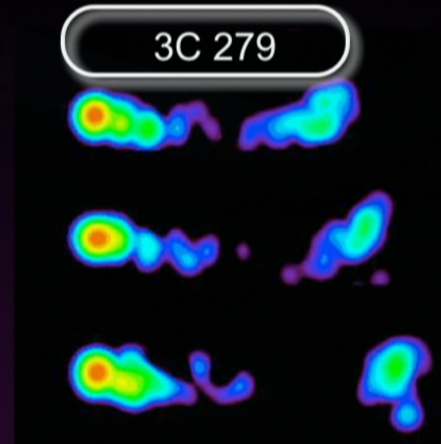


- Magnetic reconnection produces efficient and fast acceleration. This is promising to explain both the acceleration of the emitting electrons and the origin of UHECRs.

Future work:

✦ Can reconnection explain the fast variability in AGN jets?

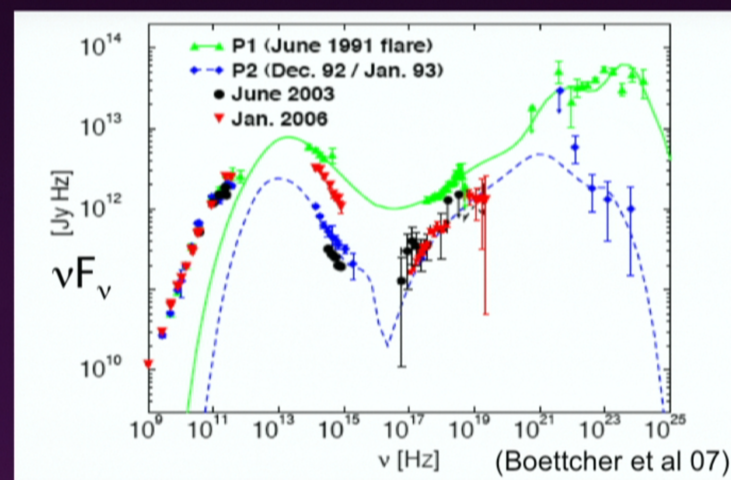


(Boettcher et al 07)

# Reconnection in Strong Gravity

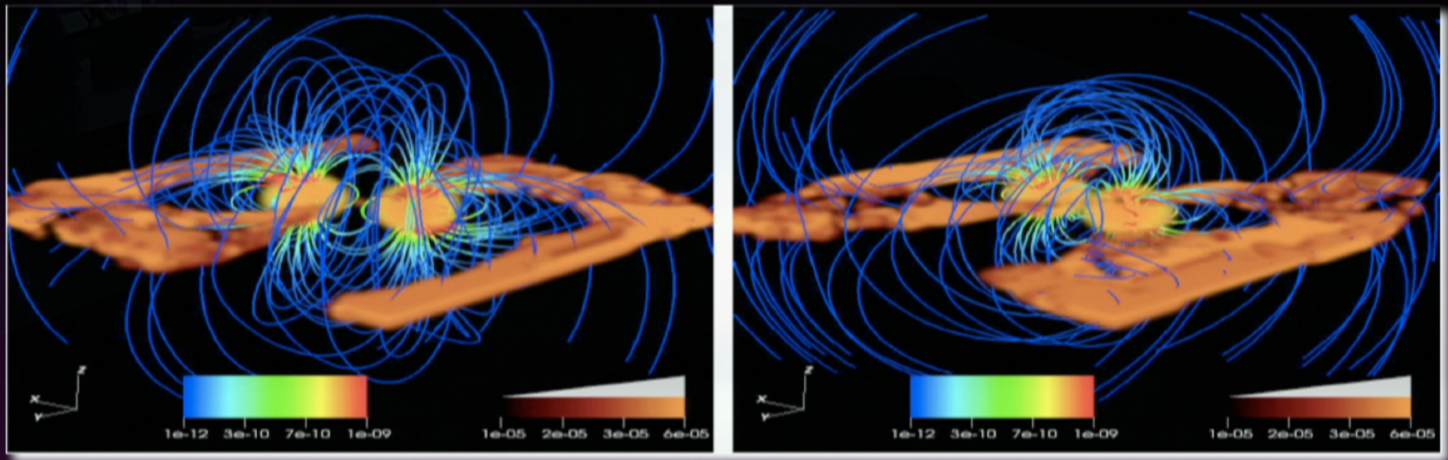


(Palenzuela et al. 13)

- Relativistic magnetic reconnection will operate in the late stages of binary neutron star mergers.

- A kinetic description is required to understand the emission signatures of relativistic reconnection. This will be important in predicting EM counterparts and precursors to gravitational wave sources.

# Reconnection in Strong Gravity

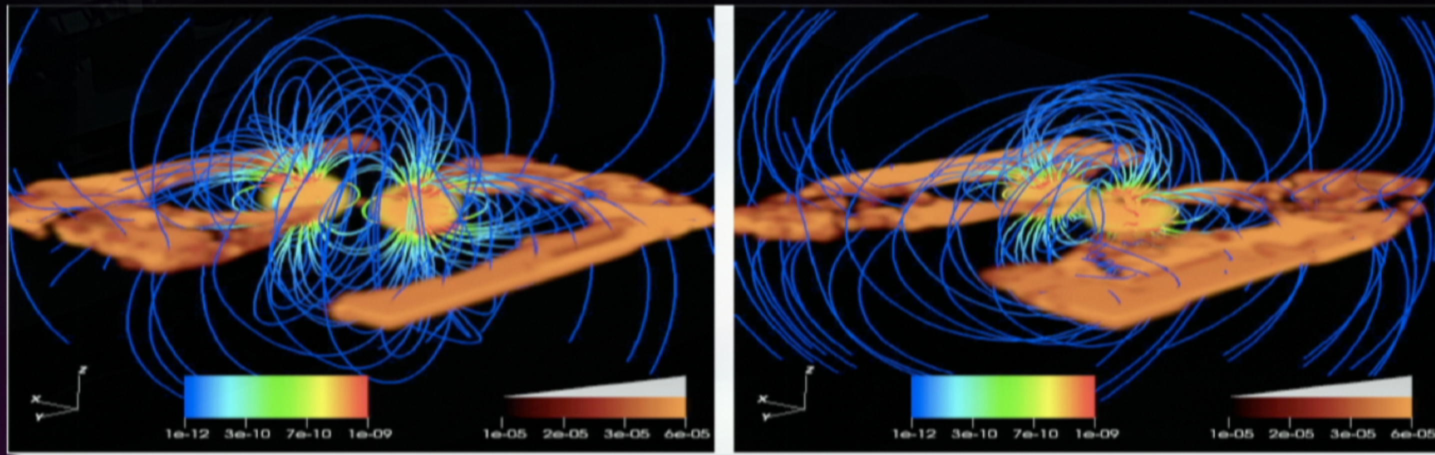


(Palenzuela et al. 13)

- Relativistic magnetic reconnection will operate in the late stages of binary neutron star mergers.

- A kinetic description is required to understand the emission signatures of relativistic reconnection. This will be important in predicting EM counterparts and precursors to gravitational wave sources.